Author for correspondence:
Ajaya Bhattarai
e-mail: bkajaya@yahoo.com

Self-assembly of sodium dodecylsulfate and dodecyltrimethylammonium bromide mixed surfactants with dyes in aqueous mixtures

K. M. Sachin[1], Sameer A. Karpe[1], Man Singh[1]
and Ajaya Bhattarai[1,2]

[1]School of Chemical Sciences, Central University of Gujarat, Gandhinagar, India
[2]Department of Chemistry, Tribhuvan University, M. M. A. M. Campus, Biratnagar, Nepal

(iD) AB, 0000-0002-2648-4686

The micellar property of mixed surfactant systems, cationic (dodecyltrimethylammonium bromide, DTAB) and anionic (sodium dodecylsulfate, SDS) surfactants with variable molar ratios in aqueous system has been reported by using surface tension and conductivity measurements at $T = 293.15$, 298.15 and 303.15 K. DTAB concentrations are varied from 1.0×10^{-4} to $3 \times 10^{-4} \, \mathrm{mol\,l^{-1}}$ in $1.0 \times 10^{-2} \, \mathrm{mol\,l^{-1}}$ SDS solution while the SDS concentration is varied from 1.0×10^{-3} to $1.5 \times 10^{-2} \, \mathrm{mol\,l^{-1}}$ in approximately $5.0 \times 10^{-3} \, \mathrm{mol\,l^{-1}}$ DTAB, so that such concentrations of DTAB-SDS (DTAB-rich) and SDS-DTAB (SDS-rich) solutions were chosen $3:1$ ratio. The critical micellar concentration, as well as surface and thermodynamic properties for DTAB-rich and SDS-rich solutions, were evaluated by the surface tension (γ) and conductivity (κ) methods. The pseudo phase separation model was coupled with the dissociated Margules model for synergism. The Krafft temperature behaviour and optical analysis of mixed surfactants are studied using conductivity and UV–Vis spectroscopy, respectively. The dispersibility and stability of DTAB-rich and SDS-rich solutions with and without dyes ($2.5 \times 10^{-5} \, \mathrm{mol\,l^{-1}}$ of methyl orange and methylene blue) are carried out by using UV–Vis spectroscopy and dynamic light scattering.

THE ROYAL SOCIETY PUBLISHING

1. Introduction

For the understanding of both fundamental and applicative prospects of mixed surfactant systems, the scrutiny of their various significant physico-chemical aspects becomes necessary. These physico-chemical aspects include aggregates formation, which depends on system environmental parameters including temperature and the other additives [1].

The physico-chemical properties (PCPs) of solutions containing both cationic and anionic surfactants, i.e. catanionic surfactant systems are different from those of their individual components. Due to the synergetic effect, the critical micellar concentration (CMC) value of mixed surfactant system is less than the pure surfactant system [2]. The catanionic surfactant system shows lower CMC, higher cloud point, lower Krafft point and higher surface activities; these properties are accommodating for their various applications [3]. At the appropriate concentrations and mole ratios, this catanionic surfactant system spontaneously tends to form fascinating structures, like mixed micelles [4], vesicles [5] and extended networks. The mixed surfactants play a very significant role in our life. It has several applications in the industrial and biological fields such as oil recovery enhancement, detergency, cosmetics, emulsification, solubilization, food industries, targeted drug delivery, wastewater treatment, chemical purification and synthesis of advanced nanomaterials [6,7]. Therefore, mixed surfactant systems are believed to be superior to single surfactant systems [8].

To date, many researchers have reported the study of micelle formation and aggregation process in the various solvent media [9,10]. The phase behaviour of various catanionic surfactant mixtures in aqueous solution is also well studied [11,12]. Among them, Zana et al. [13] studied the micellization behaviour of cationic surfactant mixtures with an aqueous solution; nevertheless, the thermodynamic properties of the solutions were not investigated. Sohrabi et al. [14] studied the phase behaviour and aggregate structures of mixed surfactants by using pulsed field gradient stimulated echo NMR technique. Yousefi et al. [15] reported the effect of co-solvent on the spontaneous formation of nanorod vesicles in catanionic mixtures of cetyltrimethylammonium bromide (CTAB) and sodium dodecylsulfate (SDS). Bhattarai [16] studied the micellization behaviour of cationic surfactant mixtures in aqueous solution as well as methyl alcohol–water mixture along with the detailed investigation of thermodynamic phenomena. Aslanzadeh & Yousefi [17] reported the micellization behaviour of tetradecyltrimethylammonium bromide (TDTAB) and SDS in the water–ethanol mixture. The self-assembling of catanionic surfactant mixtures in aqueous ionic liquid was studied by Sohrabi et al. [18]. The self-aggregation behaviour of catanionic surface active ionic liquids was studied by Xu et al. [19]. Similarly, the effect of the molecular structure of cationic surfactant mixtures on the interfacial properties at the oil–aqueous interface was reported by Wang et al. [20]. Earlier studies have been reported on the interaction of mixed surfactants with salts [21]. Recently, Bhattarai et al. [22] determined the micellar properties between DTAB and SDS in methanol–water mixed solvent media of varying proportions at 293.15 K. In this study, we have studied the effect of temperature on CMC and several other surface properties in depth; such type of study is not reported yet. Sachin et al. [23] have reported in the previous study on PCPs of DTAB-rich and SDS-rich mixed surfactant in the aqueous medium at 293.15, 298.15 and 303.15 K.

Our first objective is to determine the surface properties as the maximum surface excess concentration (Γ_{max}), area occupied per surfactant molecule (A_{min}), surface pressure at the CMC (π_{cmc}), the free energy of adsorption (G_{ads}^o), packing parameter (P), free energy of surface at equilibrium (G_{min}) and the thermodynamic properties such as the degree of ionization (α), the standard behaviour of Gibb's free energy of micellization (ΔG_m^o), enthalpy (ΔH_m^o), entropy (ΔS_m^o), heat capacity of micellization ($\Delta_m C_P^o$) of SDS-rich and DTAB-rich from γ and κ data, respectively. The study of synergistic effects of our system with the help of models is also our interest. Moreover, we study the Krafft temperature behaviour and the optical analysis of mixed surfactants by conductivity measurements and UV–Vis spectroscopy, respectively.

Earlier studies have reported the effect of dyes with single and mixed surfactants [24,25]. Samiey & Ashoori [26] have studied the kinetic and thermodynamic properties on the effect of crystal violet with DTAB and SDS. Dey et al. [27] have also reported the diffusion rate of dyes with SDS and DTAB vesicle in bulk water separately. Therefore, dye-surfactant interactions studies are very useful for industrial applications, chemical research and dye separation processes [28]. Till now, there was no literature reported yet on the effects of methylene blue (MB) and methyl orange (MO) on equimolar concentrations of SDS-rich and DTAB-rich.

Our second objective is to see the effects of each concentration of DTAB-rich surfactant with MB and MO separately and also to determine the binding and distribution constants by using the spectroscopic method as well as to estimate the stability of SDS-rich and DTAB-rich surfactant with and without dyes from dynamic light scattering (DLS) analysis.

Table 1. Comparison of measured densities values (ρ) and surface tension (γ) values of DMSO at $T = 293.15$, 298.15 and 303.15 K with the literature data. Standard uncertainties are u(T) = $\pm$ 0.01 K, u(p) = $\pm$ 0.01 MPa. Unit: $\Delta\rho = 10^3$ kg m^{-3}, $\Delta\gamma$ = mN m^{-1}. $\Delta\rho$ = Exp. - Lit., $\Delta\gamma$ = Exp. - Lit. values.

temperature (K)	$\rho/10^3$ kg m^{-3}		γ/mN m^{-1}		$\Delta\rho$	$\Delta\gamma$
	Exp.	Lit. [29]	Exp.	Lit. [30]		
293.15	1.100103	1.10073	43.41	43.36	−0.000627	0.05
298.15	1.095079	1.09574	42.78	42.70	−0.000661	0.08
303.15	1.090043	1.09074	42.12	42.05	−0.000697	0.07

2. Material and methods

2.1. Materials

The DTAB (purity approx. 99%), SDS (approx. 98.5%), MO (greater than 85%) and MB (greater than 96%) used in the experiments were obtained from Sigma-Aldrich and SD Fine Chemicals Ltd (Mumbai, India). The surfactants were stores of DTAB and SDS, the vacuum desiccator filled with P_2O_5 due to their hygroscopic nature.

2.2. Methods

Milli-Q water was used for the preparation of all the solutions of mixed surfactants at three different temperatures as described in the earlier study [23]. Also, Milli-Q water was used for the preparation of the aqueous solutions of MB and MO and stored in the airtight volumetric flasks.

2.3. Density measurements

The densities (ρ) were measured by Anton Paar DSA 5000 M density meter, which was calibrated with DMSO (table 1) at $T = 293.15$, 298.15 and 303.15 K and compared with the literature [31].

## 2.4. Surface tension measurements

The electronic counter counted the pendant drop numbers of mixed surfactants with the Survismeter [31] after attaining a thermal equilibrium in Lauda Alpha RA 8 thermostat with $\pm$ 0.05 K. The reported surface tension was average values of three repeated measurements with $\pm$ 0.03 mN m^{-1} combined uncertainty in surface tension. The Survismeter was calibrated by using DMSO. The surface tension data of our system agree well with the literature value (table 1) [30]. The presented surface tension (γ) and log C (i.e. C is the surfactant concentration) were plotted, for calculating the CMC value.

2.5. Conductance measurements

Specific conductance data were measured at $T = 293.15$, 298.15 and 303.15 K with the Pye-Unicam PW 9509 model conductivity meter having the frequency of 2000 Hz using a dip-type cell with a cell constant of 1.15 cm^{-1} with an uncertainty of 0.01%. The instrument cell was calibrated by using the proposed method [32] using the aqueous potassium chloride solution. The temperature of the measurement cell was controlled with a Lauda Alpha RA 8 thermostat with $\pm$ 0.05 K.

2.6. UV–visible spectroscopy

Absorbance was measured by the Spectro 2060 plus model of UV–visible spectrometer. The spectral analysis was done in the range of 200–600 nm at 298.15 K. All UV–visible measurements were carried out with the following procedure. Firstly, the measurement of baseline with water was done. After that, 3 ml of DTAB-rich and SDS-rich different concentrations of surfactant solutions involved obtaining a well-marked absorption band. For mixed surfactants interaction with dyes, the baseline was registered
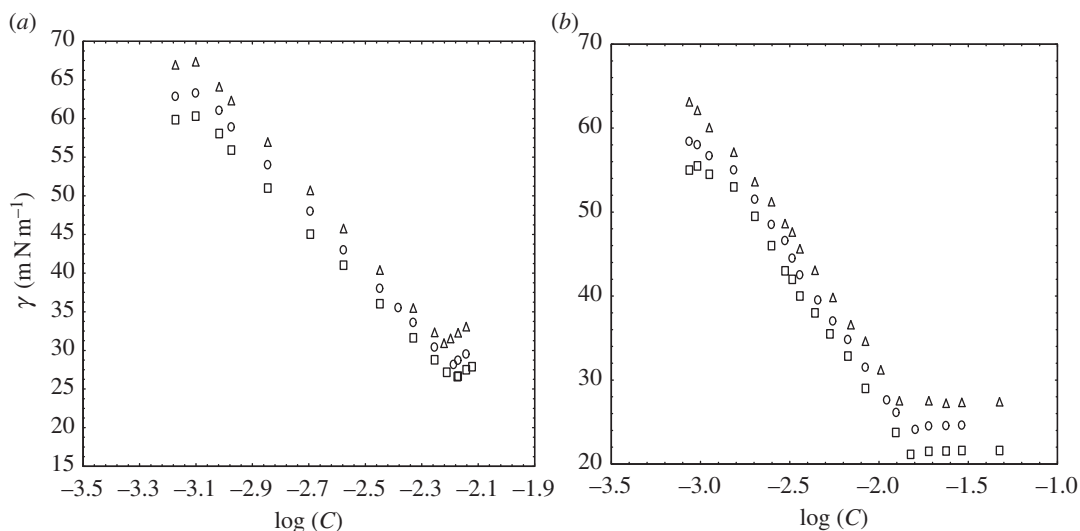
Figure 1. Plot of surface tension versus concentration of SDS-rich (*a*) and DTAB-rich (*b*) solution at $T = 293.15$ (triangle), 298.15 (circle) and 303.15 K (square).

for given DTAB-rich solution, and afterwards, a constant volume of aqueous MO or MB solution was added and the solution was mixed properly for 5 min. After that, the absorbance was noted.

By experimental data, the intensity of dye absorbance as a function of the concentration of DTAB-rich was examined. Using nonlinear regression procedure, MO and MB binding constant and MO and MB distribution constant between the aqueous phase and DTAB-rich micellar phase were calculated.

2.7. Zeta potential, polydispersity index and hydrodynamic radius measurements

Zeta potentials, polydispersity index (PDI) and hydrodynamic radius of DTAB-rich and SDS-rich surfactants in the presence and absence of MO and MB dye in the aqueous medium were measured by dynamic light scattering (DLS, MicrotracZetatrac, U2771). Using an aqueous surfactant, the set-zero was made to nullify their contribution in the formulations. The calibration was done using an aqueous dispersion of polystyrene in Milli-Q water for a standard particle diameter and zeta potential measurements at 298.15 K and $p = 0.1$ MPa with $\pm\,2$ nm and $\pm\,5$ mV uncertainties, respectively.

2.8. Krafft point measurements

The Krafft temperatures (T_K) of DTAB-rich and SDS-rich surfactant solutions were determined by placing the samples in a refrigerator at 278.15 K for at least 24 h, and the precipitation was observed. The temperature was raised slowly by recording the specific conductance after every 2 min till the steady value in the circulatory bath under constant stirring. The increment of temperature in the circulatory bath should be slow in order to make the solution homogeneous, and the mobility of the molecules of the mixed surfactants was regular, and the specific conductivity value was accurate without fluctuation in the experimental conductivity value. There was the temperature in which the specific conductance against temperature graph displayed the sudden alteration in the slope [33]. Such temperature was the same as that required for complete dissolution of the precipitated system into a clear solution. The Krafft temperature measurements reproducibility in each case was within $\pm\,0.05$ K.

3. Results and discussion

3.1. Surface tension (γ) and surface properties

We can observe in figure 1*a* that the γ initially decreases with an increment of the concentration of SDS-rich and goes to the lowest value which indicates the formation of the micelle and the break point is the CMC. Now for figure 1*b* of DTAB-rich, the γ is reduced with the sharp break after which γ stays very nearly constant. This meeting point provides CMC [34]. Table 2 contains the CMC of SDS-rich and DTAB-rich surfactant by tensiometry.

Table 2. Values of slope, critical micelle concentration (CMC), maximum surface excess concentration (Γ_{max}), area occupied by per surfactant molecule (A_{min}), surface pressure (π_{cmc}), packing parameter (P), standard free energy interfacial adsorption (ΔG^0_{ads}) of SDS-rich and DTAB-rich in aqueous medium at $T = 293.15$, 298.15 and 303.15 K. The error limits of CMC, Γ_{max}, A_{min}, π_{cmc}, P and ΔG^0_{ads} are within ± 3, ± 5, ± 4, ± 3, ± 4 and $\pm 6\%$, respectively. Standard uncertainty is $u(T) = \pm 0.01$ K.

temperature (K)	slope (mN m^{-1} lnM^{-1})	CMC (mol l^{-1})	Γ_{max} (10^6 mol m^{-2})	A_{min} (A^{02} molecule^{-1})	π_{cmc} (mNm^{-1})	P	ΔG^0_{ads} (kJ mol^{-1})
SDS-rich							
293.15	−41.70	0.0060	3.71	44.70	41.95	0.47	−43.39
298.15	−38.40	0.0063	3.36	49.37	43.85	0.43	−45.29
303.15	−37.20	0.0067	3.20	51.82	44.61	0.41	−46.31
DTAB-rich							
293.15	−32.2	0.0135	2.87	57.89	45.35	0.36	−49.5
298.15	−31.8	0.01401	2.79	59.62	47.91	0.35	−51.1
303.15	−31.3	0.0147	2.70	61.59	49.99	0.34	−52.5
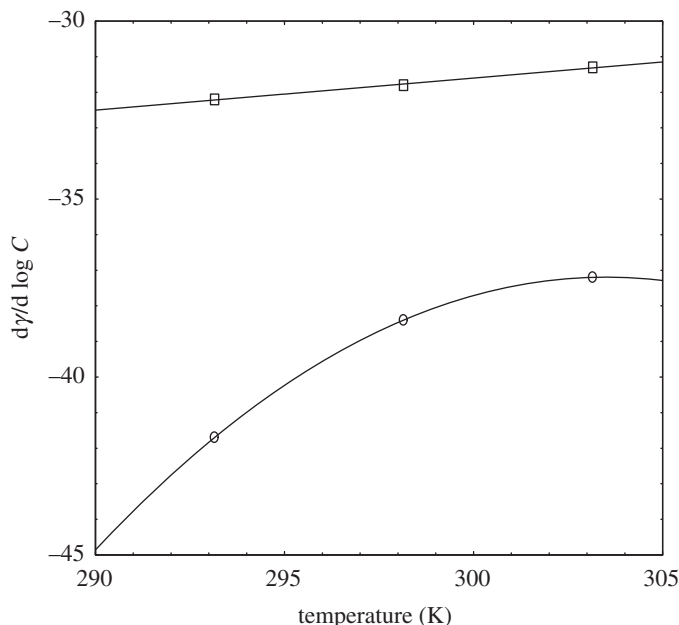
Figure 2. Variation of $(d\gamma/d\log C)$ with temperature (K) for DTAB-rich (square) and SDS-rich (circle).

The CMC of SDS-rich decreased to a value of 6.30 mM (table 2) in contrast with the CMC of 8.30 mM of SDS [35] at 298.15 K and the CMC of DTAB-rich diminished to a value of 14.01 mM (table 2) in contrast with the CMC of 14.6 mM of DTAB [36] at 298.15 K. The decrease in CMC was observed for cationic surfactant mixtures [37], due to the synergism in mixed micelle formation that is present when a mixture of two surfactants has a CMC lower than those of both individual surfactants [38]. The CMC increase here with an increase in temperature is due to the smaller probability of the hydrogen bond formation [39].

The slope $(d\gamma/d\log C)$ of the sigmoidal curve, where C is a surfactant concentration (mol l^{-1}), gives numerous facts regarding the surface properties [34]. The plot of slope $(d\gamma/d\log C)$ of SDS-rich and DTAB-rich surfactant solutions with temperature is displayed in figure 2.

The slope can play a vital role in the surface properties of mixed surfactants (table 2). It is observed in figure 2, that both the graphs containing a minimal variation in nature. For DTAB-rich, the graph is best fitted with a polynomial of second degree fit, whereas, for SDS-rich, the graph is best fitted with a linear fit. From the slope $(d\gamma/d\log C)$ of the curve, the maximum surface excess concentration (Γ_{max}) value is evaluated with Gibb's isotherm [34].

$$\Gamma_{max} = -\frac{1}{2.303nRT}\left[\frac{d\gamma}{d\log C}\right]_{T,P}. \tag{3.1}$$

Here, R is value of gas constant and n takes the value of 2 [36].

The surface excess concentration (Γ_{max}) is an adequate measure of adsorption at the air/solution interface which depends upon the nature of surfactants.

The Γ_{max} of SDS-rich in water is observed as 3.71 µmol m^{-2} (table 2) at 293.15 K which matched with the literature [22]. But there is a decrease in the value of Γ_{max} with an increase of temperature as 3.36 µmol m^{-2} (table 2) at 298.15 K in contrast with the Γ_{max} of 2.65 µmol m^{-2} of SDS in the aqueous system [35] at 298.15 K.

Similarly, Γ_{max} of DTAB-rich in water is noted as 2.87 µmol m^{-2} (table 2) at 293.15 K which agreed with the reported study [22]. But there is a decrease in the value of Γ_{max} with an increase of temperature as 2.79 µmol m^{-2} (table 2) at 298.15 K in contrast with the Γ_{max} of 1.56 µmol m^{-2} of DTAB in the aqueous system [40] at 298.15 K.

Table 2 shows that the Γ_{max} values decrease with an increase in temperature which may be due to the enhanced molecular thermal agitation at higher temperature [41]. Such behaviours were also observed in the previous study [36].

The area occupied per surfactant molecule (A_{min}) is calculated by following equation:

$$A_{min} = \frac{1}{N\Gamma_{max}}, \tag{3.2}$$

where N stands for Avogadro's number.

Our data of A_{min} value of SDS-rich in the water is 44.70 A^{o2} molecule^{-1} (table 2) at 293.15 K which is supported by the earlier result [22]. With increasing the temperature, the A_{min} value is increased as 49.37 A^{o2} molecule^{-1} (table 2) at 298.15 K, while with anionic surfactant (SDS) in water A_{min} value is 62.10 A^{o2} molecule^{-1} at 298.15 K [35].

In the same way, it is noted that the A_{min} value of DTAB-rich in water as 57.89 A^{o2} molecule^{-1} (table 2) at 293.15 K is similar to the reported data [22]. With an increase in temperature, the A_{min} value of DTAB-rich in water is observed as 59.62 A^{o2} molecule^{-1} (table 2) at 298.15 K, in contrast with the A_{min} value of DTAB in water as 106.37 A^{o2} molecule^{-1} [40] at 298.15 K.

The increase in A_{min} was observed with an increase in temperature process orientation as a result of the thermal molecular motion at high temperatures [42]. The Γ_{max} and A_{min} are inversely proportional with rising of the temperature. Such trends were also noted in earlier studies [36].

If there is no interaction [40] between SDS and DTAB, but they only compose the mixed adsorption film, the ideal area of the mixed adsorption film can be calculated as

$$A_{ideal} = \alpha, A_{min,1} + (1 - \alpha) A_{min,2}. \tag{3.3}$$

For SDS-rich, $\alpha = (0.75)$ is the mole fraction of the SDS in the total mixed solute. By substituting the values of α, $A_{min,1}$ (62.1 A^{o2} molecule^{-1} and 63 A^{o2} molecule^{-1} for pure SDS) and $A_{min,2}$ (106.37 A^{o2} molecule^{-1} and 111 A^{o2} molecule^{-1} for pure DTAB) at 298.15 K and 303.15 K, respectively, in equation (3.3), we get A_{ideal} (73.16 A^{o2} molecule^{-1} at 298.15 K and 75 A^{o2} molecule^{-1} at 303.15 K).

Similarly, For DTAB-rich, $\alpha = (0.75)$ is the mole fraction of the DTAB in the total mixed solute. By substituting the values of α, $A_{min,1}$ (106.37 A^{o2} molecule^{-1} and 111 A^{o2} molecule^{-1} for pure DTAB) and $A_{min,2}$ (62.1 A^{o2} molecule^{-1} and 63 A^{o2} molecule^{-1} for pure SDS) at 298.15 K and 303.15 K, respectively, in equation (3.3), we get A_{ideal} (95.30 A^{o2} molecule^{-1} at 298.15 K and 99 A^{o2} molecule^{-1} at 303.15 K).

It is observed that the values of A_{ideal} are higher than A_{min} of SDS-rich and DTAB-rich systems (table 2), and the values of A_{ideal} are higher than A_{min} of DTAB and SDS. Also, it is noted that the A_{min} values for SDS-rich and DTAB-rich systems are lower in comparison with the pure SDS and DTAB. Such behaviour was noted in the literature [40]. The lowered A_{min} values indicate a significant attractive interaction between the components of the mixed surfactant system and hence the strongest attraction between the oppositely charged head groups [43].

The surface pressure at the CMC (π_{cmc}) is calculated by using the following equation:

$$\pi_{cmc} = \gamma_o - \gamma_{cmc}, \tag{3.4}$$

where γ_o and γ_{cmc} have the usual meanings.

The calculated π_{cmc} value of SDS-rich in water as 41.95 mN m^{-1} (table 2) at 293.15 K closed with the literature [22]. With an increase in temperature, the π_{cmc} value is also increased as 43.85 mN m^{-1} (table 2) at 298.15 K, but there is the difference in π_{cmc} of SDS in water as 32.43 mN m^{-1} at 298.15 K [35].

Similarly, the π_{cmc} value of DTAB-rich in water is found as 45.35 mN m^{-1} (table 2) at 293.15 K and then closed with an already reported study [22]. With an increase in the temperature, the π_{cmc} value is obtained as 47.91 mN m^{-1} (table 2) at 298.15 K which is different from the π_{cmc} value of DTAB in water as 29.35 mN m^{-1} [40] at 298.15 K.

An increase in π_{cmc} is observed with an increase in temperature. The reason is that π_{cmc} is a measure of the efficiency of the surfactant to lower the surface tension of water. Such increase in π_{cmc} with a rise in temperature was also noted in the earlier research work [44]. Normally, an increase in π_{cmc} for mixed surfactants deals with an associative interaction [45]. Israelachvili *et al.* [46] have discussed the micellar shape. To find out the packing parameter, the surface area of amphiphiles in mixed micelles and micellar growth may be used as

$$P = \frac{V_o}{A_{min}l_c}. \tag{3.5}$$

The value of P as 0.47 of SDS-rich in the aqueous system (table 2) at 293.15 K is similar to the literature data [22]. But with increase in the temperature, the P value decreases as 0.43 (table 2) at 298.15 K in contrast with the value as 0.34 for P of SDS in water at 298.15 K [35]. Similarly, P of DTAB-rich in water is observed as 0.36 (table 2) at 293.15 K is close to the literature [22], and when temperature increases, there is a decrease in the P value as 0.35 (table 2) at 298.15 K in contrast with the P value as 0.20 at 298.15 K of DTAB in water [36].
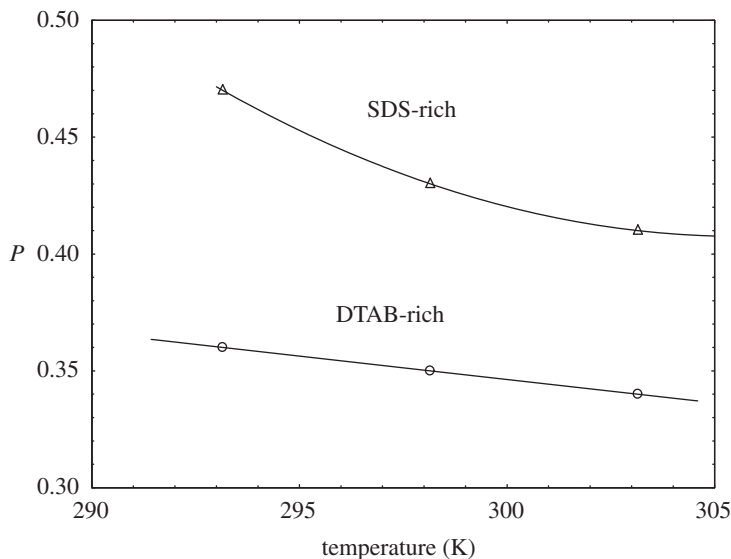
Figure 3. Variation of P with temperature (K).

Thus, the packing parameter infers that the structural parameter of the surfactant at a molecular level with a favoured interfacial curvature is the resulting aggregate. The geometry of surfactant indicates that with the deep impact in the type of self-assembly structure of surfactants formed in solution, which is dependent on the packing parameter, amphiphiles can form different structures, spherical, cylindrical micelles, lamellar phases and reverse micelles, etc. [47].

Basically, the micelles are spherical for $p < 1/3$, cylindrical for $p < 1/2$ suggested by Israelachvili *et al.* [46]. In our investigation, from table 2, it is observed that P values for both DTAB-rich and SDS-rich are higher than 0.3, indicating the formation of cylindrical or rod-shaped micelles. With an increasing temperature, the P values decrease due to inducing the vibrational, rotational and translational oscillations with wreaking of binding forces of the SDS-rich and DTAB-rich mixed surfactants system [41]. Such a trend was also seen in the reported study [36]. The higher value of P in mixed surfactants indicates disc-like micelles formation in water, which should also be suitable to form reverse micelles [48].

3.1.1. Correlation of packing parameter with temperature

The decrease of P with temperature is sharply linear having a correlation coefficient ($r^2 = 1$) for DTAB-rich whereas SDS-rich shows the decrease of P with temperature is in the concave pattern curve (figure 3).

From Tanford's formula [49], V_0 is the volume of exclusion per monomer in the micelle:

$V_0 = [27.4 + 26.9n_c)]\mathring{A}^3$, $l_c = [1.54 + 1.26(n_c)]\mathring{A}$; l_c is the highest chain length, whereas n_c is carbon atoms in the chain of a hydrocarbon. The free energy of adsorption was calculated by using the following equation [46]:

$$\Delta G^o_{ads} = \Delta G^o_m - \frac{\pi_{cmc}}{\Gamma_{max}}. \tag{3.6}$$

From equations (3.1)–(3.6), Γ_{max}, A_{min}, π_{cmc}, P and G^o_{ads} are evaluated for DTAB-rich and SDS-rich and are displayed in table 2.

Our data of ΔG^o_{ads} of SDS-rich in water is observed as $-43.39 \text{ kJ mol}^{-1}$ (table 2) at 293.15 K and it is similar to the reported value [22], while at 298.15 K, the ΔG^o_{ads} value decreases as $-45.29 \text{ kJ mol}^{-1}$ (table 2) of SDS-rich system, and the value of $-51.80 \text{ kJ mol}^{-1}$ for ΔG^o_{ads} of SDS in aqueous system at 298.15 K was observed [40].

In the case of DTAB-rich in water, the ΔG^o_{ads} value is $-49.5 \text{ kJ mol}^{-1}$ at 293.15 K and then it is closed with the literature [22]. With an increasing temperature, the ΔG^o_{ads} value decreases as $-51.1 \text{ kJ mol}^{-1}$ (table 2) at 298.15 K in contrast with the value of $-48.63 \text{ kJ mol}^{-1}$ for ΔG^o_{ads} of DTAB in an aqueous system at 298.15 K [36].

Negative values of ΔG^o_{ads} indicate spontaneity of the adsorption of surfactant molecules on the surface. The ΔG^o_{ads} values become more negative on increasing the temperature, which is indicating
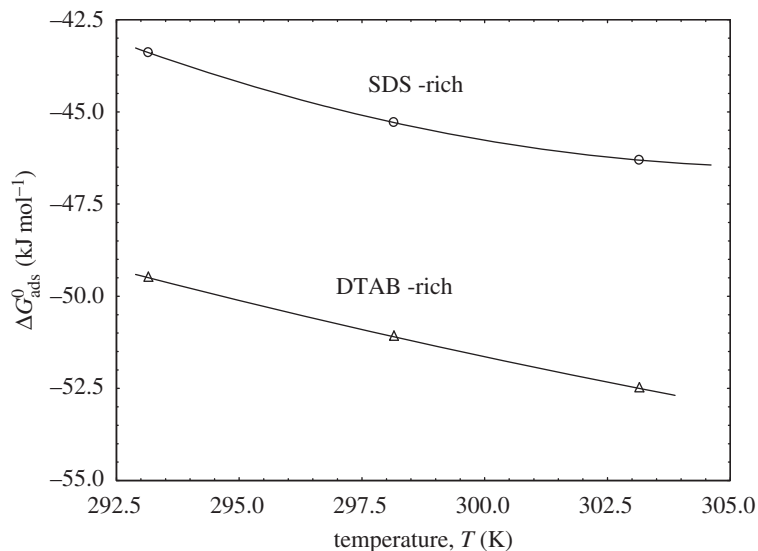
Figure 4. Variation of ΔG^o_{ads} with temperature (K).
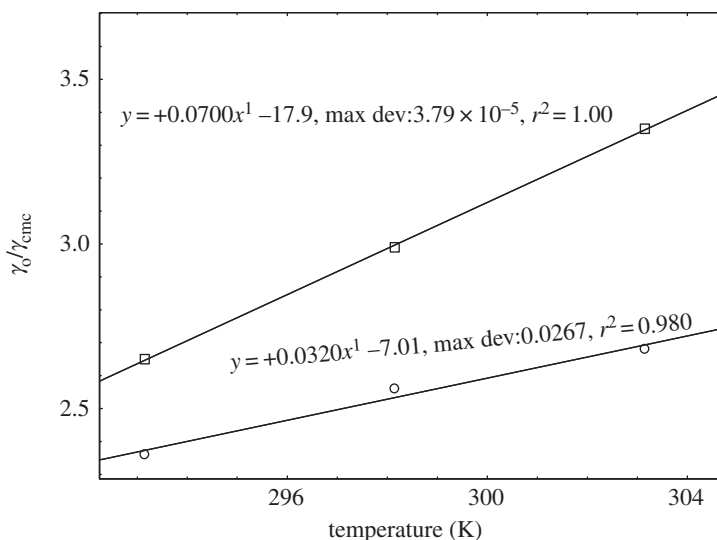
Figure 5. Variation of γ_0/γ_{cmc} with temperature: open circles (SDS-rich) and open squares (DTAB-rich).

the higher spontaneity of adsorption of surfactant molecules on the surface; the negative ΔG^o_{ads} values were also observed in the literature [36].

3.1.2. Correlation of ΔG^o_{ads} with temperature

Gibbs energies of adsorption of SDS-rich and DTAB-rich show the unique variation. It is found that there is a concave curve with an increase of temperature for SDS-rich, whereas, in DTAB-rich, the curve became linear with a correlation coefficient ($r^2 = 1$) with an increase of temperature (figure 4).

3.1.3. Correlation of γ_0/γ_{cmc} with temperature

Secondary parameters can be generated from the primary data of surface tension. In 2012, a new concept to describe the solvophobic effect [50] was proposed by Mukhim and Ismail. They calculated the ratio of the solvent surface tension to the solution surface tension at the CMC, γ_0/γ_{cmc}. This ratio can be used to describe the solvophobic effect [51]. Figure 5 shows that the variation of the ratio of the solvent surface tension to the solution surface tension at the CMC with temperature for DTAB-rich and SDS-rich systems. The plot of γ_0/γ_{cmc} with the volume fraction of methanol at 293.15 K was noted for the concave nature of the curves by Pathak *et al.* [22] for DTAB-rich and SDS-rich systems, whereas we have seen the linear

Table 3. Values of solution surface tension (γ_{cmc}), solvent surface tension (γ_o), γ_o/γ_{cmc}, free energy of surface at equilibrium (G_{min}) and $\Delta G^o_{ads}/\Delta G^o_m$ of SDS-rich and DTAB-rich in aqueous medium at $T = 293.15$, 298.15 and 303.15 K. Errors limits of γ_{cmc}, γ_0 and ΔG_{min} are within $\pm$ 4%, $\pm$ 3% and $\pm$ 5%, respectively.

temperature (K)	γ_{cmc} (mN m^{-1})	γ_o (mN m^{-1})	γ_o/γ_{cmc}	G_{min} (kJ mol^{-1})	$\Delta G^o_{ads}/\Delta G^o_m$
SDS-rich					
293.15	30.80	72.75	2.362	8.29	1.35
298.15	28.16	72.01	2.557	8.37	1.40
303.15	26.60	71.21	2.677	8.30	1.43
DTAB-rich					
293.15	27.40	72.75	2.655	9.55	1.47
298.15	24.10	72.01	2.988	8.65	1.50
303.15	21.16	71.21	3.349	7.85	1.54

variation with temperatures for DTAB-rich and SDS-rich systems. But the DTAB-rich has the higher curve than SDS-rich with a slope (0.07) and the correlation coefficient ($r^2 = 1$) and whereas SDS-rich has a slope (0.032) and the correlation coefficient ($r^2 = 0.980$).

The observed ΔG^o_{ads} values are higher than ΔG^o_{min} values indicating the adsorption at the air–solution interface is more favourable than the formation of micelles in the bulk solution [52]. The ratio of $\Delta G^o_{ads}/\Delta G^o_m$ was found to be approximately 1.5 (table 3) for SDS-rich and DTAB-rich at different temperatures indicating less spontaneity in the transfer of the monomers to the interface [53].

Free energy of surface at equilibrium is also known as molar Gibbs energy at CMC for maximum adsorption attained. This is one of the thermodynamic parameters for the evolution of synergism in mixed adsorption film at equilibrium [54] and calculated as follows:

$$G_{min} = A_{min} \, \gamma_{cmc} N_A, \tag{3.7}$$

where γ_{cmc} is the surface tension at CMC and N_A is the Avogadro's number. We observed the lower values of G_{min} in SDS-rich and DTAB-rich systems. The observed lower values of G_{min} ascertain the thermodynamic stability [55]. Since the obtained G_{min} values are lower in magnitude (table 3), it can be inferred that thermodynamically stable surfaces are formed with synergistic interaction [56].

As we have two systems (DTAB-rich and SDS-rich) and their interaction is discussed at three different temperatures above, different parameters from surface tension are studied. Here we want to take one representative system as DTAB-rich and compare with DTAB at 303.15 K by some parameters. Here, 21.16 is the γ_{cmc} for DTAB-rich at 303.15 K (table 3), and 39 was the γ_{cmc} of DTAB at 303.15 K [57]. The Γ_{max} for DTAB-rich at 303.15 K is 2.70 (table 2), and 1.51 was the Γ_{max} of DTAB at 303.15 K [57]. The A_{min} for DTAB-rich at 303.15 K is 61.59 (table 2), and 111 was the A_{min} of DTAB at 303.15 K [57]. The CMC for DTAB-rich at 303.15 K is 14.7 mM (table 2), and 15.3 was the CMC of DTAB at 303.15 K [57]. Thus we can say from the above comparison that the addition of DTAB into SDS leads to the strong electrostatic attraction between (+ve and −ve) charged head groups and the strengthening of the interaction between the SDS and DTAB molecules, thus leading to larger Γ_{max}, smaller A_{min} and lower CMC and γ_{cmc} at air/solution interface [58].

The further detailed investigation regarding the interaction between DTAB and SDS is also carried out in the following section by conductivity study.

3.2. Specific conductance measurement and thermodynamic properties

The specific conductance of the mixture of DTAB and SDS in the form of DTAB-rich and SDS-rich solutions in water for the calculation of the CMC at $T = 293.15$, 298.15 and 303.15 K are displayed in electronic supplementary material, figure S1. The specific conductance values of DTAB-rich and SDS-rich system increases with increment in temperature. The conductivity increases with increment in concentration with a certain slope. However, at a particular concentration, the slope changes for each plot. The break of two straight lines is indicated as the CMC. A degree of ionization (α) can be obtained from the ratio of post-micellar (S_2) to the pre-micellar slope (S_1). The variations in pre- and post-micellar slopes on the plots of conductance with a concentration of the solution of DTAB-rich and SDS-rich solutions in the mixed surfactants are given in table 4. With an increase of temperature,

Table 4. Values of pre-micellar slope (S_1), post-micellar slope (S_2), degree of ionization (α), critical micelle concentration (CMC), Gibb's free energy of micellization (ΔG_m^o), standard enthalpy of micellization (ΔH_m^o), the standard entropy of micellization (ΔS_m^o) of SDS-rich and DTAB-rich in an aqueous medium at $T = 293.15$, 298.15 and 303.15 K. The error limits of CMC, α, ΔG_m^o, ΔH_m^o and ΔS_m^o are within ± 4, ± 4, ± 4, ± 5 and $\pm 5\%$, respectively. Standard uncertainty is $u(T) = \pm 0.01$ K.

temperature (K)	S_1 (mS cm^{-1} M^{-1})	S_2 (mS cm^{-1} M^{-1})	α	CMC (mol l^{-1})	ΔG_m^o (kJ mol^{-1})	ΔH_m^o (kJ mol^{-1})	ΔS_m^o (J mol^{-1} K^{-1})
SDS-rich							
293.15	64.5	36.3	0.56	0.00592	−32.096	−9.876	75.7945
298.15	62.28	35.5	0.57	0.00620	−32.25	−10.040	74.4887
303.15	58.97	34.2	0.58	0.00650	−32.38	−10.459	72.3316
DTAB-rich							
293.15	105.0	35.8	0.34	0.01349	−33.67	−10.425	79.2864
298.15	100	35.0	0.35	0.01400	−33.88	−10.73	77.6400
303.15	94.4	34.1	0.36	0.01470	−34.03	−11.053	75.7985
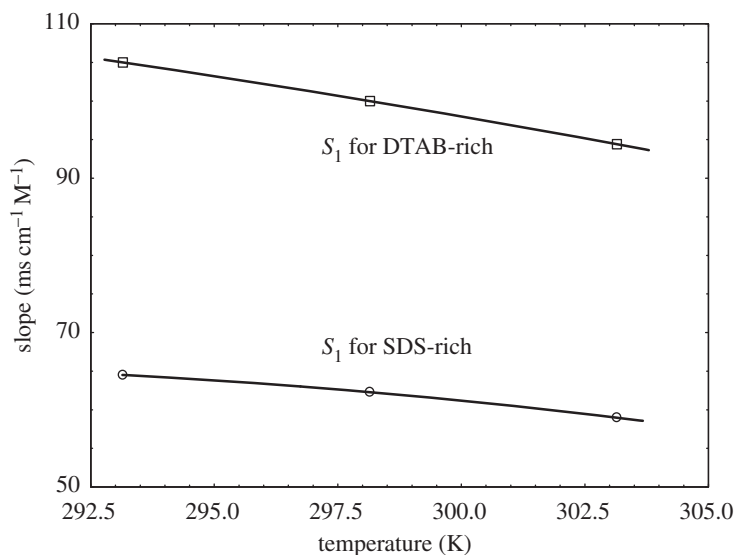
Figure 6. Variation of slope versus temperature in pre-micellar slope regions.
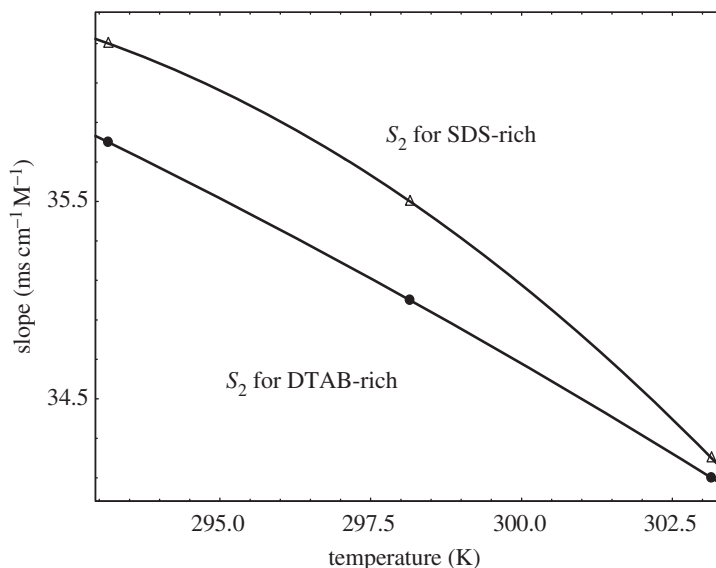
Figure 7. Variation of slope versus temperature in post-micellar slope regions.

both slopes (pre-CMC and post-CMC) decrease (table 4 and figures 6 and 7) for DTAB-rich and SDS-rich systems. But pre-micellar slopes decrease monotonously showing almost linear variation for DTAB-rich and SDS-rich systems and the post-micellar slopes decrease sharply showing almost linear variation for DTAB-rich, and the nature of the curve seems convex for SDS-rich system.

The mixed surfactants have shown the largest pre-CMC slopes and smallest post-CMC slopes leading to the lowest degrees of dissociation (table 4). These slopes are so sensitive, which decides the degrees of dissociation, CMC and other thermodynamic parameters.

The CMC obtained for DTAB-rich and SDS-rich system from conductivity measurements in water at three different temperatures are given in table 4. It indicates that the CMC increases with increasing temperature. The effect of temperature on micelle formation could be explained by two reasons. The first reason is as the temperature increases, the degree of hydration of the hydrophilic group decreases, which could favour micelle formation; however, a rise in the temperature also induces disruption of the water structure surrounding the hydrophobic group, and this is unfavourable to micelle formation. It seems from the data of table 4 that the second effect is a main studied temperature range [59].

The CMC of SDS-rich diminished to a value of 6.2 mM (table 4) in contrast with the CMC of 8.38 mM of SDS [60] at 298.15 K, and CMC of SDS-rich is observed as 6.5 mM (table 4) at 303.15 K in contrast with the CMC of 8.5 mM of SDS [61] at 303.15 K, while the CMC of DTAB-rich diminished to a value of

14.00 mM (table 4) in contrast with the CMC of 14.50 mM of DTAB [36] at 298.15 K and the CMC of DTAB-rich is observed as 14.70 mM (table 4) at 303.15 K in contrast with the CMC of 15.1 mM of DTAB [57] at 303.15 K by conductivity methods. Herrington *et al.* [62] observed the decrease in CMC for cationic surfactant mixtures. Such a decline in CMC happens in the more substantial synergistic effects between two oppositely charged surfactants that are mixed homogeneously.

3.2.1. Synergistic effects

The synergistic effects can be observed with the help of models. The synergism in the mixed surfactants is possible when the CMC of a mixture is less than that of individual surfactants among the mixture. So, we have selected our SDS-rich system for the study of synergistic effects because, in DTAB-rich system, the values of mixed CMCs are found to be lower than the CMC values of pure DTAB and higher than the CMC values of pure SDS. Moreover, we have tested the values for β^m (the micellar interaction parameter) of DTAB-rich and SDS-rich systems from the conductivity study with the famous equations given in the literature [38] as

$$x^2 \ln\left(\alpha \frac{CMC}{xCMC_1}\right) \Big/ (1-x)^2 \ln\left[\frac{(1-\alpha)CMC}{(1-x)CMC_2}\right] = 1 \tag{3.8}$$

and

$$\beta^m = \ln\left(\alpha \frac{CMC}{xCMC_1}\right) \Big/ (1-x)^2. \tag{3.9}$$

For SDS-rich, CMC = CMC of mixed surfactant system for SDS-rich system, CMC_1 = CMC of pure SDS for SDS-rich system and CMC_2 = CMC of pure DTAB for SDS-rich system. The α and x are the mole fractions of the SDS in the total mixed solute and the mixed micelles, respectively.

Similarly, for DTAB-rich, CMC = CMC of mixed surfactant system for DTAB-rich system, CMC_1 = CMC of pure DTAB for DTAB-rich system and CMC_2 = CMC of pure SDS for DTAB-rich system. The α and x are the mole fractions of the DTAB in the total mixed solute and in the mixed micelles, respectively.

We found that β^m was positive for DTAB-rich system as 0.5677 at 293.15 K, 0.8077 at 298.15 K and 0.8284 K at 303.15 K, by solving equation (3.8) iteratively to obtain the value of x and then putting the value of x into equation (3.9), whereas the negative values of β^m were found for SDS-rich system (table 5). The evaluated positive and negative values of β^m for DTAB-rich and SDS-rich systems were used in Rubingh's equations (3.10) and (3.11) to calculate the activity coefficients (γ_1 and γ_2). DTAB-rich systems generated values greater than 1 for γ_1 and γ_2, whereas SDS-rich systems produced values less than 1 for γ_1 and γ_2.

$$ln\gamma_1 = \beta^m(1-x)^2 \tag{3.10}$$

and

$$ln\gamma_2 = \beta^m x^2. \tag{3.11}$$

As the values of γ_1 as well as γ_2 in aqueous as well as other media in the entire study, α are less than unity, showing the synergistic interactions as well as non-ideal behaviour of the mixed systems [63].

So, DTAB-rich system explains the antagonistic interaction whereas SDS-rich system explains synergistic interaction. Therefore, we proceeded with further investigations on SDS-rich system.

The obtained values of γ_1 and γ_2 were less than 1, so the Clint condition of ideality was not recovered. So, we used our data to calculate the mixed CMC from the equation

$$\frac{1}{CMC} = \frac{\alpha}{\gamma_1 \; CMC_1} + \frac{1-\alpha}{\gamma_2 \; CMC_2}. \tag{3.12}$$

Thus obtained mixed CMC values were lower than the measured experimental CMC of our system (tables 4 and 5) even though β^m were the negative values (table 5). So, we used the pseudo phase separation model coupled with the dissociated Margules model [21] and obtained the almost closer mixed CMC in comparison with the experimental mixed CMC (tables 4 and 5 and figure 8).

The interesting facts are that the Margules model used equations (3.13) and (3.14) if $A_{12} = A_{21} = \beta^m$, then equations (3.13) and (3.14) recover to equations (3.10) and (3.11).

$$ln\gamma_1 = [\, A_{12} + 2(A_{21} - A_{12})\, x](1-x)^2 \tag{3.13}$$

and

$$ln\gamma_2 = [\, A_{21} + 2(A_{12} - A_{21})\, (1-x)]x^2. \tag{3.14}$$
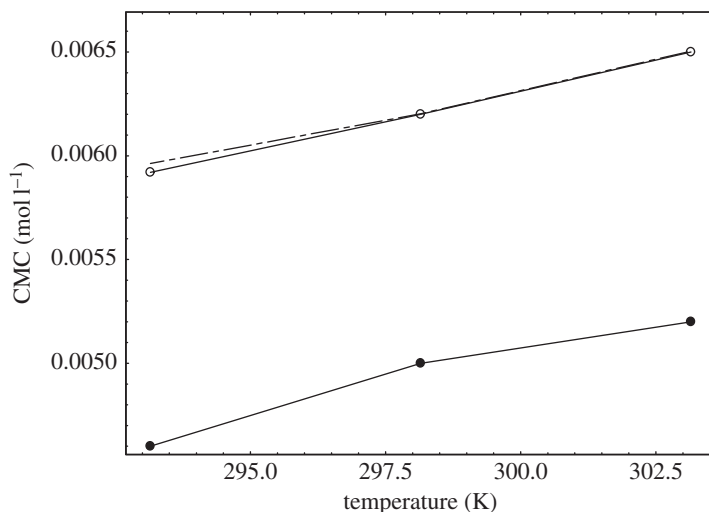
Figure 8. Variation of CMC versus temperature: closed circles: calculated CMC values from Rubingh model; open circles: experimental CMC values from the conductivity study; dashed lines are the CMC values from the dissociated Margules model.

Table 5. Values of β^m, critical micelle concentration (CMC) from Rubingh model and dissociated Margules model, A_{12} and A_{21} of SDS-rich in aqueous medium at $T = 293.15$, 298.15 and 303.15 K.

temperature (K)	β^m	CMC from Rubingh model (mM)	CMC from Margules model (mM)	A_{12}	A_{21}	CMC of SDS CMC_1 (mM)	CMC of DTAB CMC_2 (mM)
293.15	−2.727	4.61	5.96	−1.70	−3.897	8.03[a] [60]	15.38[a] [64]
298.15	−2.450	5.07	6.20	−1.65	−3.088	8.38[a] [60]	14.50[a] [36]
303.15	−2.436	5.16	6.50	−1.51	−3.681	8.5[a] [61]	15.1[a] [57]

[a]Conductivity methods.

By using possible dissociation in SDS-rich system, then equations (3.13) and (3.14) can be changed into

$$ln\gamma_{1,r_1} = [\, A_{12} + 2(A_{21} - A_{12})\, x_{,r_1}]\, (1 - x_{,r_1})^2 \tag{3.15}$$

and

$$ln\gamma_{1,r_2} = [\, A_{21} + 2(A_{12} - A_{21})\, (1 - x_{,r_1})]x_{,r_1}^2. \tag{3.16}$$

The details about these two parameters (A_{12} and A_{21}) as well as γ_{1,r_1}, γ_{1,r_2} and $x_{,r_1}$ were described in the literature [21]. Then for the above SDS-rich systems, A_{12} and A_{21} were iteratively evaluated with the help of equations (3.13)–(3.16) and are given in table 5.

The value of $(r_1A_{12} + r_2A_{21})/ (r_1 + r_2)$ is equivalent to β^m when cationic and ionic surfactant mixed at equimolar composition and β^m acts as a measure of the excess interaction between the two different surfactants in mixed micelles. Here, we suppose that surfactant SDS generates r_1 particles, and surfactant DTAB generates r_2 particles. It was found in the literature [21] that for the near-symmetric DTAB/SDS/H$_2$O mixed system, the two surfactants DTAB and SDS had the same alkyl chain and similar surface activities, their interaction was useful for the complete dissociation of surfactants, both r_1 and r_2 were chosen as 2 and observed more negative values of A_{12} and A_{21}; whereas, in our SDS-rich system, we have used r_1 and r_2 as 1 instead of 2, because r_1 and r_2 as 2 generated the positive values of A_{12} and A_{21} which is in contrast with synergistic effects.

By using $r_1 = r_2 = 1$ in our system, we get the value of A_{12} and A_{21} less negative in comparison with the literature [21]. That may be one of the reasons we observed different values of A_{12} and A_{21}, and other reason may be that we used asymmetrical amounts of SDS and DTAB. Hao et al. [21] used almost the symmetrical amount of SDS and DTAB, which interact highly by generating more negative values of

A_{12} and A_{21}, whereas our SDS-rich system gives less negative values of A_{12} and A_{21} as SDS is more in excess in the mixture, which lowers the value of r_1 and r_2. Such types of behaviour were also discussed in the literature [65]. When the deviation is more, the degree of interaction between the mixed systems is higher. Hence the positive deviation as in our DTAB-rich system explains the antagonistic interaction, while the negative deviation as in our SDS-rich indicates the synergistic interaction. Therefore, there is still a need to have a huge research scope for the mixed micellization of opposite charged surfactants [66].

The free energies of micelle formation are calculated by a pseudo-phase separation model [22] and given in table 4.

$$\Delta G_m^o = (2 - \alpha)RT \, lnX_{cmc}, \tag{3.17}$$

where X_{cmc}, R and T have the usual meanings.

The value of α for SDS-rich in water is noted to be 0.56 (table 4) at 293.15 K and closed with the literature [22]. When the temperature has increased, the value of α is increased as 0.57 (table 4) at 298.15 K, but α of SDS in water was noted as 0.45 [67] at 298.15 K.

In the same way, the α value for DTAB-rich in water is noted as 0.34 (table 4) at 293.15 K and similar to the previously reported study [22]. But α of DTAB-rich in water is observed as 0.35 (table 4) at 298.15 K whereas α of DTAB in water as 0.21 was noted in the literature [36] at 298.15 K, and α of DTAB-rich is observed as 0.36 (table 4) at 303.15 K in contrast with the α of 0.29 of DTAB [57] at 303.15 K.

The increase in α with temperature is because of the decreasing charge density on the micellar surface. A more significant fraction of the counterions is dissociated and increasing the temperature reduces the aggregation number of the ionic surfactants [68].

The data of ΔG_m^o for SDS-rich in water is found as -32.096 kJ mol^{-1} (table 4) at 293.15 K, which is similar to the earlier studied work [22], and an increase of temperature shows the free energy formation is more negative as -32.25 kJ mol^{-1} (table 4) at 298.15 K in contrast with the ΔG_m^o value for SDS in water as -34.04 kJ mol^{-1} [67] at $T = 298.15$ K, and ΔG_m^o of SDS-rich is observed as -32.38 kJ mol^{-1} (table 4) at 303.15 K in contrast with the ΔG_m^o of -36.2 kJ mol^{-1} of SDS [61] at 303.15 K.

In the case of DTAB-rich in water, ΔG_m^o is -33.67 kJ mol^{-1} (table 4) at 293.15 K and a similar result was noted in the earlier study [22], and an increase of temperature shows the free energy formation is more negative as -33.88 kJ mol^{-1} (table 4) at 298.15 K in contrast with the ΔG_m^o value for DTAB in water as -35.25 kJ mol^{-1} [69] at 298.15 K, and ΔG_m^o of DTAB-rich is observed as -34.03 kJ mol^{-1} at 303.15 K (table 4) in contrast with the ΔG_m^o of -35.73 kJ mol^{-1} of DTAB [69] at 303.15 K.

The ΔG_m^o is negative with all systems and becomes more negative as the temperature increases (table 4). The higher negative ΔG_m^o with increasing temperature indicates that the micellization process is spontaneous and becomes more spontaneous with an increase in temperature. Our results are also supported by the literature [70]. The decreasing value of ΔG_m^o is attributed to the tendency to drive equilibrium towards hydrophobic bonding as temperature increased. Furthermore, the free energy of micelle formation is more negative in DTAB-rich systems in contrast to the SDS-rich systems at investigated temperatures whereas the free energy of micelle formation is less negative in DTAB-rich and SDS-rich systems in comparison to pure DTAB and SDS at investigated temperatures. Less negative ΔG_m^o indicates co-solute does not facilitate the micellization.

Standard enthalpies of micelle formation, the ΔH_m^o value is calculated by the Gibbs–Helmholtz equation as

$$\Delta H_m^o = -RT^2(2 - \alpha)\left[\frac{\partial lnX_{cmc}}{\partial T}\right]_P \tag{3.18}$$

by fitting the graph of lnX_{cmc} against temperature, and then the term $\left[\frac{\partial lnX_{cmc}}{\partial T}\right]_P$ is calculated. ΔS_m^o can be evaluated with the help of ΔG_m^o and ΔH_m^o by the following equation (3.19):

$$T\Delta S_m^o = \Delta H_m^o - \Delta G_m^o. \tag{3.19}$$

Our data of ΔH_m^o for SDS-rich in water is obtained as -9.876 kJ mol^{-1} (table 4) at 293.15 K and increase of temperature shows ΔH_m^o is more negative as -10.04 kJ mol^{-1} (table 4) at 298.15 K while the ΔH_m^o value for SDS in water as -14.49 kJ mol^{-1} was noted in the literature [67] at $T = 298.15$ K. In the case of DTAB-rich in water, ΔH_m^o is -10.425 kJ mol^{-1} (table 4) at 293.15 K and increase of temperature shows ΔH_m^o is more negative as -10.73 kJ mol^{-1} (table 4) at 298.15 K whereas the value of ΔH_m^o for DTAB in water was -9.08 kJ mol^{-1} [69] at 298.15 K, and ΔH_m^o of DTAB-rich is observed as -11.053 kJ mol^{-1} (table 4) at 303.15 K in contrast with the ΔH_m^o of -9.38 kJ mol^{-1} of DTAB [69] at 303.15 K.

Table 4 shows that the micellization is exothermic at $T = 293.15$, 298.15 and 303.15 K for the DTAB-rich and SDS-rich system. Hence, ΔH_m^o is negative with all systems and becomes more negative as the temperature increases (table 4). It depicts the decrease in energy required for breaking the iceberg structure surrounding the alkyl chains of DTAB-rich and SDS-rich. Also, ΔH_m^o is more negative in DTAB-rich systems in comparison with pure DTAB, whereas in SDS-rich systems at 298.15 K, ΔH_m^o is less negative in comparison with pure SDS. Less negative value of ΔH_m^o may be due to an increase of hydrophobic interaction.

In our study of DTAB-rich and SDS-rich system, DTAB-rich are highly exothermic, primarily because of tail association [71]. Negative enthalpy values infer the importance of London dispersion interactions (LDI) as an attractive force for micellization for DTAB-rich and SDS-rich system [72]. The negative values of enthalpies of micellization for DTAB/SDS mixtures at 303.15 K found from microcalorimetry [73] also support our findings of enthalpies of micellization.

Our calculated data of ΔS_m^o for SDS-rich in water is found as 75.7945 J mol^{-1} K^{-1} (table 4) at 293.15 K and decreases with increasing the temperature as 74.4887 J mol^{-1} K^{-1} (table 4) at 298.15 K, whereas the value of ΔS_m^o for SDS in water as 65.67 J mol^{-1} K^{-1} was mentioned [67] at 298.15 K. With DTAB-rich in water, ΔS_m^o is 79.2864 J mol^{-1} K^{-1} (table 4) at 293.15 K, and increase of temperature shows ΔS_m^o decreases as 77.6400 J mol^{-1} K^{-1} (table 4) at 298.15 K, while the ΔS_m^o value for DTAB in water as 87.8 J mol^{-1} K^{-1} [69] at 298.15 K and ΔS_m^o of DTAB-rich is observed as 75.7985 J mol^{-1} K^{-1} (table 4) at 303.15 K, in contrast with the ΔS_m^o of 87 J mol^{-1} K^{-1} of DTAB [69] at 303.15 K. Moreover, the values of ΔS_m^o in DTAB-rich solutions were observed to be high, in contrast to the SDS-rich solutions at investigated temperatures.

On increasing the temperature, the ΔS_m^o value decreases for DTAB-rich and SDS-rich system. It may be because of the disruption of the iceberg water structure around the alkyl group with increasing the kinetic energy of the system.

In our study, we observed the positive value of ΔS_m^o with DTAB-rich and SDS-rich systems. It infers that a liquid–phase aggregate could be formed, whereas a negative value of ΔS_m^o may indicate the formation of the solid–phase aggregate [71].

Therefore, the negative values of ΔH_m^o and ΔG_m^o and positive values of ΔS_m^o are indicative for DTAB and SDS interactions. Such behaviour is also noted in the earlier study [74]. But in the literature [71], the negative values of entropy have been reported.

Electronic supplementary material, figure S2 shows the relationship of enthalpy–entropy compensation phenomenon for DTAB-rich and SDS-rich in the water at $T = 293.15$, 298.15 and 303.15 K. A linear relationship is obtained for $\Delta H_m^o - \Delta S_m^o$ and is expressed with the help of the following equation:

$$\Delta S_m^o = \frac{1}{T_c}\Delta H_m^o + \sigma, \tag{3.20}$$

where $1/T_c$ is slope and σ are intercepts of a linear plot. T_c measures solvation part of micellization while σ determines the solute–solvent interaction. T_c values obtained in water for DTAB-rich and SDS-rich are 179.86 K and 172.71 K, respectively. ΔG_m^o, ΔH_m^o and ΔS_m^o of DTAB-rich and SDS-rich in water at $T = 293.15$, 298.15 and 303.15 K are displayed in table 4, whereas the values of T_c, σ and $\Delta_m C_p^o$ for DTAB-rich and SDS-rich solutions by using conductivity measurement are given in table 6.

The heat capacity of micellization ($\Delta_m C_p^o$) which is obtained from the slope of ΔH_m^o against temperature curve (electronic supplementary material, figure S3) is noted as

$$\Delta_m C_p^o = \frac{\partial \Delta_m H^o}{\partial T}. \tag{3.21}$$

The negative value of the heat capacity of micellization ($\Delta_m C_p^o$) is observed for the self-association of amphiphiles.

3.3. UV–visible absorption spectroscopy

3.3.1. Optical analysis

Systematic UV–Vis spectroscopic investigations of DTAB-rich and SDS-rich solutions were carried out to understand the behaviour of mixed surfactants association in water. The absorption maxima of an aqueous solution of DTAB-rich were found at 210 nm and 280 nm, respectively (figure 9).

With increasing the concentration of DTAB into aq-SDS initially, the absorbance intensity is increased significantly due to the hyperchromic shift as for 0.005 M DTAB only; the maximum absorbance of 2.377
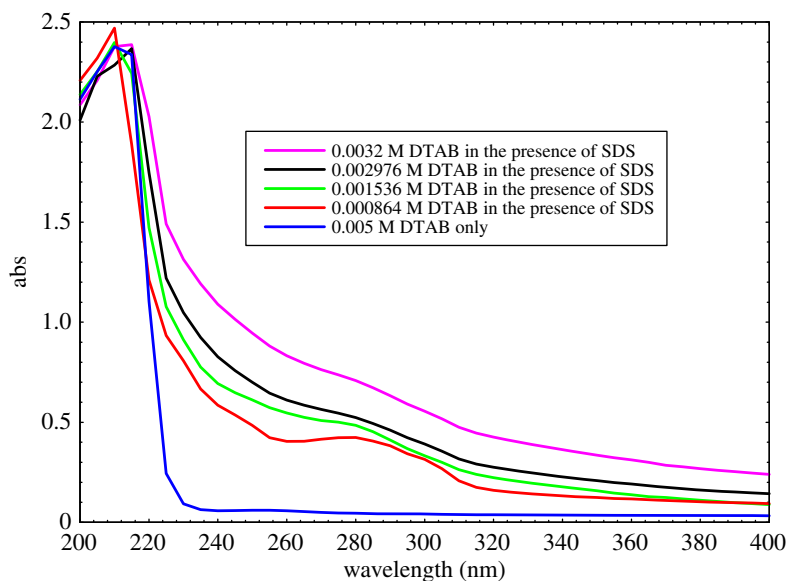
Figure 9. Absorption spectra of DTAB-rich surfactant.

Table 6. Compensation parameters: T_c, σ and $\Delta_m C_p^o$ value of SDS-rich and DTAB-rich by using conductivity measurement.

| compensation parameters	SDS-rich	DTAB-rich
$T_c(K)$	172.71	179.86
σ	132.8	137.2
$\Delta_m C_p^o$ (J mol^{-1} K^{-1})	-58.2	-62.8

at 210 nm is noted. When adding the constant amount of 0.01 M SDS in 0.000864 M DTAB, the absorbance increases up to 2.469 without red or blue shift, but only the hyperchromic shift is observed. When the amount of DTAB increases up to 0.001536 M in the constant concentration of 0.01 M SDS, i.e. the absorbance decreases as 2.398, so there is the observation of hypochromic shift. Further, adding more DTAB as 0.002976 M with 0.01 M SDS, there is the observation of hypochromic shift as well as red shift containing absorbance as 2.367 at 215 nm, and again on increasing the concentration of DTAB as 0.0032 M with 0.01 M SDS, there is the observation of hyperchromic shift containing absorbance as 2.387 at 215 nm, while at 280 nm the hyperchromic shift is observed with increasing DTAB concentration due to the weakening of binding forces, van der Waals forces and electrostatic interaction. The results depicted that the hydrophobic interactions among surfactant tails also give rise to the higher adsorption of surfactant molecules. Such behaviour was also observed for cationic-rich and anionic-rich mixtures of CTAB and SDS in the literature [75].

The absorption maxima of an aqueous solution of SDS-rich were found at 270 nm and 360 nm, respectively (figure 10).

With increasing the concentration of SDS into aq-DTAB initially, the absorbance intensity is increased significantly due to the hyperchromic shift as for 0.01 M SDS only; the maximum absorbance of 0.039 at 270 nm is noted. When adding the constant amount of 0.005 M DTAB into 0.000096 M SDS, the absorbance increases up to 0.248 without red or blue shift but only hyperchromic shift is observed. When the amount of SDS increases up to 0.00048 M in the constant amount of 0.005 M DTAB, i.e. the absorbance also increases as 0.424, the observation is a hyperchromic shift. On further adding more SDS as 0.000672 M to 0.00096 M with 0.005 M DTAB, there is the observation of hyperchromic shift for both cases as 0.597 and 0.768 absorbances. In the same manner, for 360 nm, there is also absorbance of 0.01 for 0.01 M SDS only. When the constant DTAB is added as 0.005 M in 0.000096 M SDS, there is the progressive evolution of the absorbance bands as 0.169 at 360 nm. In the case of 0.00048 M, 0.000672 M and 0.00096 M SDS, the constant amount of 0.005 M DTAB interacts with SDS solutions to give the absorbance of 0.346, 0.401 and 0.449, respectively. Hence, two visible peaks at 270 and 360 nm of SDS-rich surfactant mixture give only the hyperchromic shift, but not visible blue
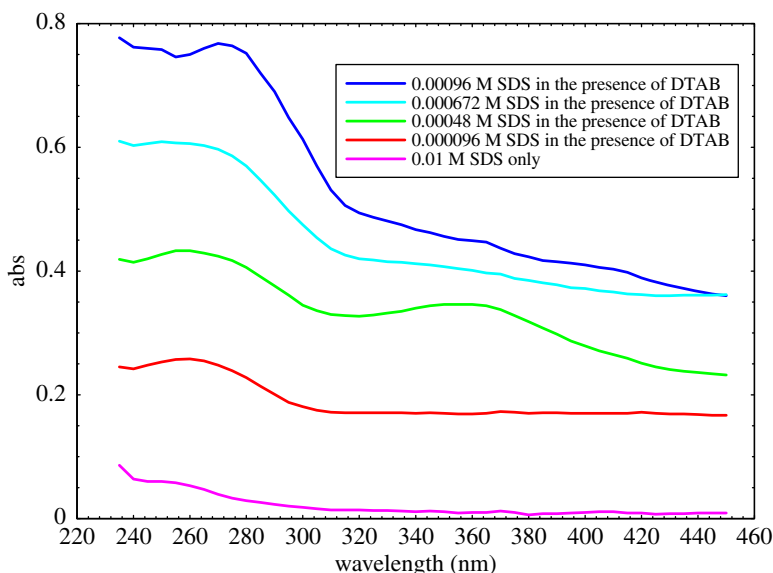
Figure 10. Absorption spectra of SDS-rich surfactant.
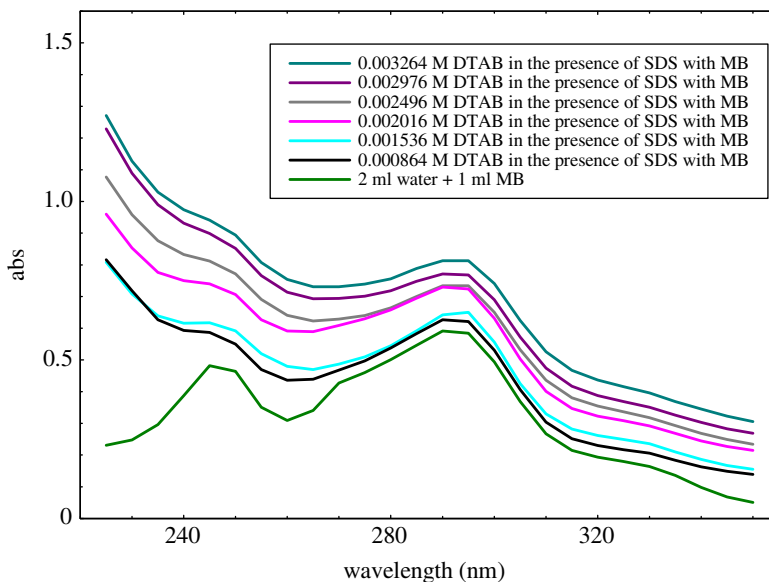
Figure 11. Absorption spectra of DTAB-rich surfactant in the presence of MB.

or red shift is noted at the investigated concentrations of SDS solution in the presence of DTAB. Thus, our results show that the hydrophobic interactions among surfactant tails give rise to the higher adsorption of surfactants molecules. Liu *et al.* have also been observed such type of behaviour of variable concentration of SDS in the aqueous medium [76]. Our findings of SDS-rich surfactant mixtures are also supported from the literature [24].

3.3.2. Interaction between dyes and mixed surfactants

Figure 11 shows that the absorbance intensity of the MB in aqueous solution affected with increasing the DTAB concentration. Thus, the MB and DTAB have positive charges while with SDS is opposite so they could be induced to have a weak interaction with the hyperchromic shift. With increasing the concentration of surfactants, the maximum MB molecules could be accommodated into normal micelles as monomeric molecules, and absorbance intensity sharply increases with the hyperchromic shift [77].
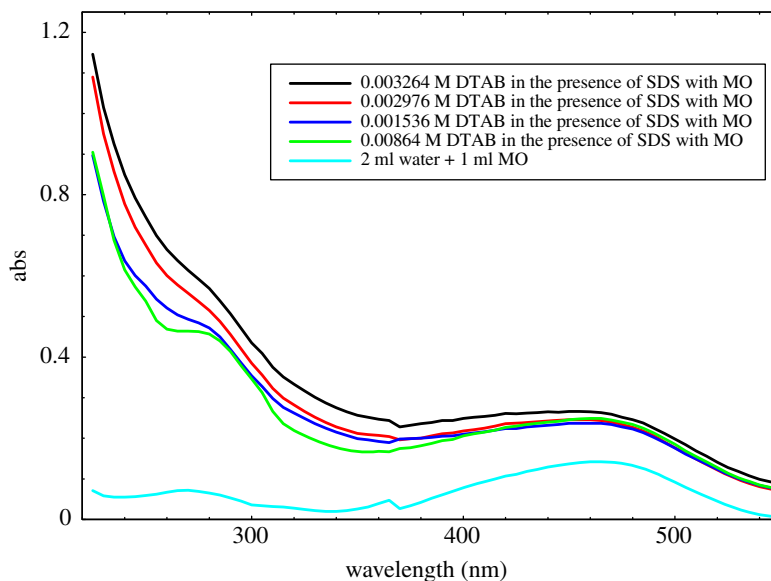
Figure 12. Absorption spectra of DTAB-rich surfactant in the presence of MO.

Figure 12 shows that the absorption peaks are obtained from MO in the aqueous medium. Such characteristic of the MO could be used for studying the DTAB-rich surfactants aggregates in the aqueous medium. The influences of different concentration of DTAB on the absorption spectrum of MO were studied by using UV–Vis spectroscopy. On increasing the concentration of DTAB, the absorbance intensity increases monotonously with the hyperchromic shift, which could induce strong interaction between MO and DTAB-rich solution as compared to MB with DTAB-rich solution. Our patterns of spectra are also supported by the reported study [78]. In the case of DTAB-rich with MB and MO solution showing more hydrophobic micellar environment, the maximum absorbance of dyes with surfactants is observed. In the case of SDS-rich interaction with MB and MO solution, there was cloudy in the preparation of the solutions. Two intense absorption bands were registered between 275 and 465 nm for MO, and between 245 and 295 nm for MB, which is in good agreement with the literature data [79,80], as shown in figures 11 and 12.

Moreover, there is a progressive evolution of these bands with an increase of DTAB-rich concentration. The interaction of MO and MB with DTAB-rich has non-visibly shifted (figures 11 and 12). By assuming the ideal behaviour of dye in both phases, the distribution constant of dye following Nernstian distribution law can be written as

$$K = \frac{m_{\mathrm{m}}}{m_{\mathrm{o}}}. \tag{3.22}$$

Here, K is distribution constant, whereas m_{m} and m_{o} are the concentrations of dye in micellar and aqueous phases. In the analysis of spectra of UV–Vis, parameter A was calculated. Following Magid et al. [81], the ratio of dye absorbance's band intensities (A) was described as a function of cationic rich surfactant concentration and A value is a sum of two parameters,

$$A = x_{\mathrm{m}}A_{\mathrm{m}} + (1 - x_{\mathrm{m}})A_{\mathrm{o}}, \tag{3.23}$$

where x_{m} is the dye mole fraction, A_{m} is the value of A corresponding to the situation when dye completely dissolves in micellar phases, whereas A_{o} related to aqueous phases. In our case, dyes dissolve in pure water so the distribution constant can be presented as

$$K = \frac{n_{\mathrm{m}}}{n_0[\mathrm{DTAB} - \mathrm{SDS}]M_{\mathrm{DTAB-SDS}}}, \tag{3.24}$$

where n_{m} is the moles of dye in aqueous phase whereas n_0 is with micellar phases, the [DTAB-SDS] is the molarity of DTAB in the presence of SDS, and the $M_{\mathrm{DTAB-SDS}}$ is molecular weight of DTAB in the presence of SDS. Following the procedure developed in the literature [81] on analysis of the UV–Vis

Table 7. The fitting parameters (A_m and K') obtained in the nonlinear regression procedure (NLREG) of the UV–Vis data for dyes partitioning between water and (DTAB-SDS) micelles measured at room temperature and K (distribution constant) calculated from relation: ($K' = K * M_{DTAB-SDS}$).

S.N.	A_m^a	K' (binding constant) [l mol^{-1}]	K (distrib. constant)
	methyl orange (MO)		
1.	0.4290	21200	68753.48
	methylene blue (MB)		
2.	0.0116	126	408.6300

[a]Absorbance of dyes dissolved in micellar phase.

spectra, the binding constant K' of dye to reversed micelle is given as

$$K' = \frac{n_m}{n_0[\text{DTAB} - \text{SDS}]}. \tag{3.25}$$

There is a connection between K and K' as $K' = K * M_{DTAB-SDS}$.

According to Poisson distribution [59], equation (3.25) can be written as

$$x_m = \frac{K'[\text{DTAB} - \text{SDS}]}{1 + K'[\text{DTAB} - \text{SDS}]}. \tag{3.26}$$

Combining equations (3.23) and (3.26), we get

$$A = A_o + \frac{(A_m - A_o)K'[\text{DTAB} - \text{SDS}]}{1 + K'[\text{DTAB} - \text{SDS}]}. \tag{3.27}$$

Here A_m and K' were fitted parameters, A_o values were found in a separate experiment. Obtained results are presented in electronic supplementary material, figures S4 and S5. Fitted parameters and constant distribution values are summarized in table 7. Table 7 indicates that the stronger interactions between MO with DTAB-rich micelles appeared in comparison among MB with DTAB-rich micelles.

3.4. Zeta potential, polydispersity index and hydrodynamic radius measurement for stability analysis

The ξ is a potential that exists among the particle surface and dispersing liquid which changes according to the distance from the particle surface. The greater the positive/negative charge of the ξ, the more stable the particles are (due to electrical repulsion). Nevertheless, the higher ξ value describes the higher dispersed condition of the particle in an aqueous media. For an adsorbent, a large available surface area is desirable, which is possible if it has been in dispersed condition (higher ξ value). The ξ and hydrodynamic radius (R_h) values of DTAB-rich and SDS-rich surfactants with and without MO and MB with an aqueous medium have been determined. The ξ, R_h and PDI values (table 8) reflect the dispersion and stability of the solution. The higher ξ value indicates the higher repulsive strength of molecules [82]. Our study found the higher positive ξ value (27.02 mV) with MB + water system, whereas the lower ξ value (0.53 mV) with 0.005 M DTAB+MB system; similarly, a higher negative ξ values -15.13 with 0.012 M SDS + 0.005 M DTAB, while the lower ξ value -0.54 with MO + water system.

The PDI is a dimensionless parameter. If the PDI values are less than 0.05, it means that the solution has a high monodispersity, while for greater than 0.7, it indicates that the solution has a polydispersive nature [83]. The interaction between MB and SDS indicates that MB is encountering a microenvironment in the SDS micelles. Probably, the SDS-MB form stable solution which could be induced by both coulombic and hydrophobic interactions [84], and the interaction of MB [85] with SDS could proceed by the mechanism opposite to that of micelle formation. In our study, MB and SDS concentrations being unchanged, the initially clear, homogenous solution becomes opalescent. Similar changes (appearance of opalescence) were also observed in ageing of initially homogeneous SDS-MB solutions, suggesting that the system is thermodynamically and kinetically stable. So, SDS-MB is strongly monodispersive with highly dispersive solutions. In the case of DTAB-rich samples as 0.005 M DTAB + MB, 0.005 M DTAB + MO are also highly monodispersive with strongly stable and highly dispersive solutions.
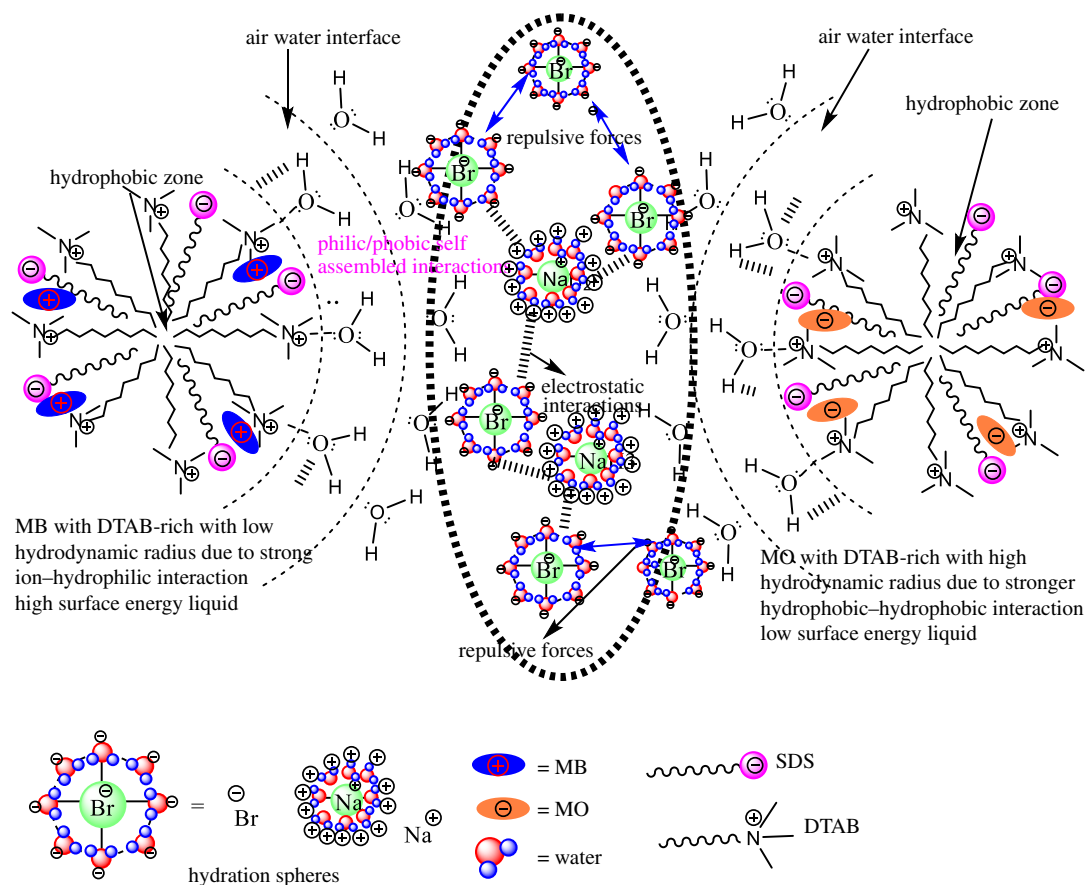
Figure 13. Molecular structural interactions of MO and MB with DTAB-rich mixed surfactants.

Table 8. Zeta potential (ξ), hydrodynamic radius (R_h) and PDI value of DTAB-rich and SDS-rich in the presence and absence of MB and MO at 298.15 K.

| systems	R_h (nm)	PDI	ξ (mV)
SDS-rich			
0.01 M SDS	3640	1.201	0.57
0.012 M SDS + 0.005 M DTAB + MB	3720	1.170	−11.10
0.01 M SDS + MB	5230	0.1152	1.75
MO + water	5160	0.2680	−0.54
0.01 M SDS + MO	4650	1.784	0.56
0.012 M SDS + 0.005 M DTAB	3270	1.708	−15.13
0.012 MSDS + 0.005 M DTAB + MO	3630	0.706	−13.75
DTAB-rich			
0.005 M DTAB	2355	1.589	0.55
0.00504 M DTAB + 0.01 M SDS + MB	3530	1.0310	12.59
0.005 M DTAB + MB	4660	0.392	0.53
MB + water	4780	1.846	27.02
0.005 M DTAB + MO	5350	0.2394	0.55
0.00504 M DTAB + 0.01 M SDS	5990	2.285	14.18
0.00504 M DTAB + 0.01 M SDS + MO	6000	2.481	−9.15
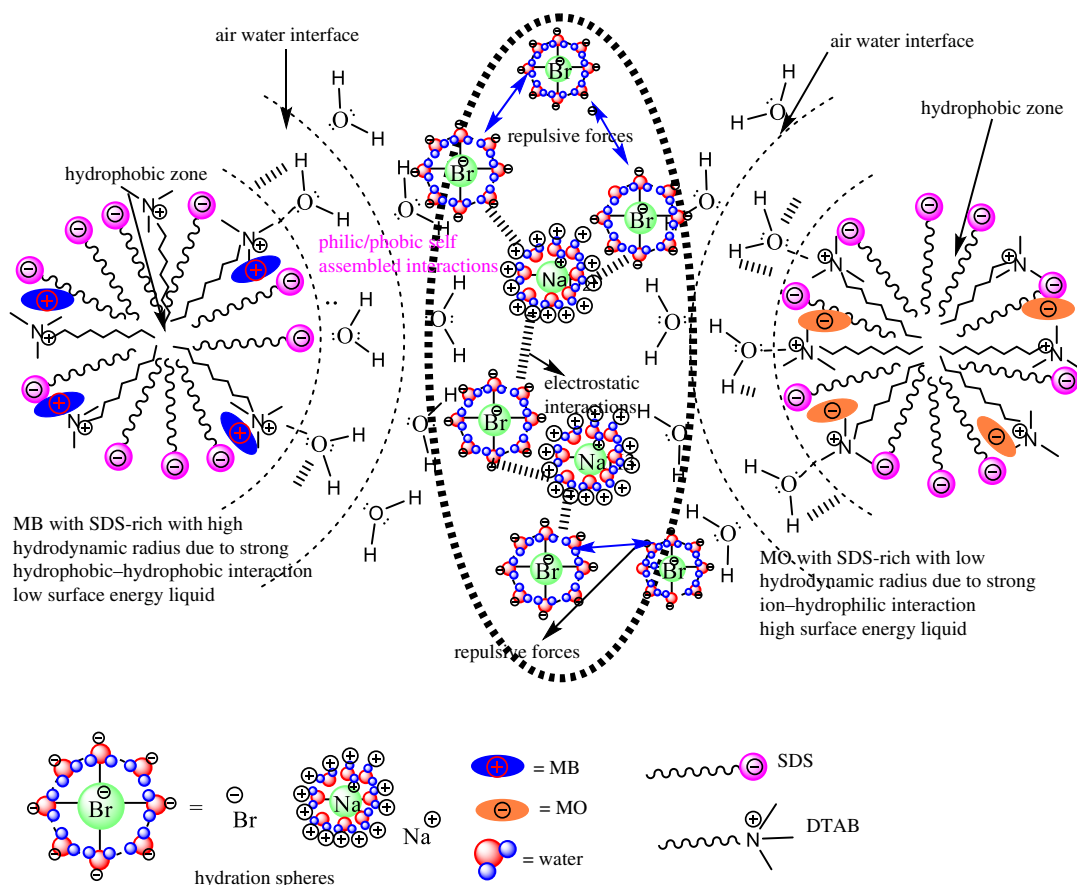
Figure 14. Molecular structural interactions of MO and MB with SDS-rich mixed surfactants.

Similarly, the interaction mechanism could be developed in the DTAB-MO system; DTAB and MO depict that the stronger electrostatic interactions for positive part of quaternary ammonia of DTAB and negative part of a sulfonate group of the MO with hydrophobic interactions could be induced in the electrostatic and ion-phobic/philic interactions with DTAB-MO system. The maximum PDI value is 2.481 for 0.00504 M DTAB + 0.01 M SDS + MO and the minimum PDI value is 0.2394 for 0.005 M DTAB + MO.

The surfactants and dyes are developed in an individual hydration sphere in the solution. Due to the stronger electrostatic, ion-dipole and intermolecular interaction, this could be started as the formation of stable dye-surfactant solution due to such interaction; the dyes are arranged like H-type aggregation [86]. It depicted that the dye-surfactant is a monomer with the electrostatic interaction among positive part of the quaternary nitrogen of DTAB and negative part of sulphonate group, and the alkyl chain length (ACL) of DTAB strongly interacts with azo-group (chromophoric unit) of the rest of the molecules of MO dye [87]. Moreover, lots of factors such as mobility and dispersivity play an essential role in the dye–surfactant interaction. The H-type aggregation of MO with DTAB molecules in the liquid mixture and also different types of aggregates could be dependent on the ACL. The methylene groups ($-CH_2-$) in the ACL could affect the interacting and packing parameters of dye-surfactant in the aqueous medium. The hydrophobic nature of ACL also has an important impact on the DTAB aggregation. Thus, the ion–hydrophobic, electrostatic and ion–dipole interactions (IDI) in between dye and surfactants micelles play a significant part in the penetration of dye into micelles and the solubilization and distribution of the dye molecules between aqueous and micellar phases. Table 8 shows that the SDS-rich system 0.012 M SDS + 0.005 M DTAB has (3270 nm) the lowest hydrodynamic radius due to the stronger electrostatic interaction and intermolecular forces, while the 0.005 M DTAB system shows a stronger interaction with solvent molecules. The DTAB-rich system 0.00504 M DTAB + 0.01 M SDS + MO has (6000 nm) the highest hydrodynamic radius. It depicts that due to the ion–hydrophobic interaction dominant over IHI.

Figure 13 shows that an addition of MB into DTAB-rich mixed surfactant shows weak interaction because DTAB and MB have same charges, due to the dominant ion-hydrophilic interaction (IHI) over the ion-hydrophobic interaction (IH_bI) with decreasing R_h value. Similarly, with MO into DTAB-rich, the R_h value is increased with strong hydrophobic-hydrophobic interaction (H_bH_bI).
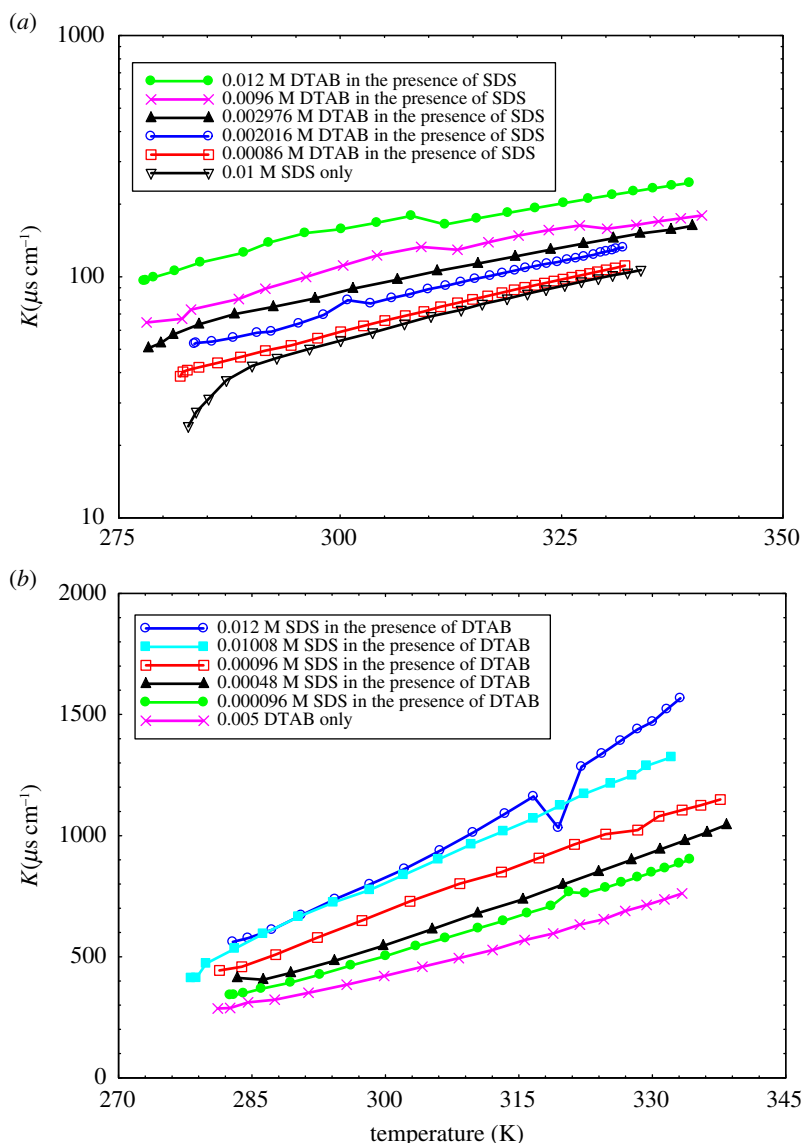
Figure 15. Conductivity (κ) versus T/K for Krafft temperature (T_K) of (*a*) DTAB-rich and (*b*) SDS-rich surfactants.

MB with SDS-rich mixed surfactant (figure 14) shows strong H_bH_bI because SDS and MB have phobic/philic nature, it could be induced by weak electrostatic interaction and increased the R_h value with high surface energy liquids, while with MO into SDS-rich (figure 14), the R_h value is decreased because of strong electrostatic interaction and multiple intermolecular interactions. On addition of SDS and DTAB into aq-DTAB and aq-SDS solution, the increased R_h size of mixed surfactant is apparently increased as the size of aggregates increased (table 8) and also, by a DLS experiment wherein the R_h value of the DTAB-rich and SDS-rich were observed to increase in the presence of MO and MB dyes (table 8). This is in contrast to the stability of the R_h in the absence and presence of dyes with a mixed surfactant system. In our study, we observed an inclusion of MO and MB into SDS-rich and DTAB-rich mixed surfactant; the R_h is increased as well as aggregation increases with the higher stability of the solution. The systems containing ionic dyes and surfactants charged opposite to the dye electrostatic interactions develop. As a result of the attraction forces, ionic pairs dye-surfactant (MB and MO with DTAB-rich and SDS-rich) are formed in a stable solution [88]. Hydrophobic interactions, electrostatic interactions, hydrogen bonds, p-stacking and Van der Waals forces are typical examples of the intermolecular forces that dominate the interactions of dye molecules with surfactant aggregates [89].

3.5. Krafft point measurements

The Krafft point is generally the interaction between the solubility and CMC of the surfactant [18]. With increasing temperature, the solubility is increased. The solubility is adequate to the CMC at a particular

temperature, and hence the micelles can form [90]. The solubility and CMC curves intersect at the specific temperature called the Krafft temperature (T_K). Figure 15 of SDS-rich and DTAB-rich were measured by the use of κ data in the aqueous medium [88].

The degree of counterion dissociation of ionic micelles is calculated from T_K measurements. T_K of DTAB and SDS are the roles of the counterions concentration in water. When the aqueous solution of ionic surfactant goes above the saturation concentration, a hydrated solid surfactant stage is divided [89]. The solubility is determined at temperatures below the Krafft point. The micelles begin to form at the Krafft point. The Krafft point can be determined as the temperature at which the solubility versus temperature curve intersects. Zhang *et al.* [91] have reported Krafft point and the solubility of SDS only on the function of temperature. By the use of the third-order polynomial equation, the relationship between solubility and temperature of surfactants has been determined. Gayet *et al.* [92] have studied the temperature effect on CMC value for SDS. An addition of MB and MO into SDS-rich and DTAB-rich mixed surfactant could induce electrostatic interactions; multiple intermolecular interactions (IMMI) form the stable thermodynamic solution. Although for cationic-anionic combinations a high probability of precipitation through change neutralization at comparable ratio is present, when one component is increased, the stably mixed micelles are usually formed [93]. However, in this study, we have chosen 3 : 1 critical ratio of surfactants; at this ratio surfactants do not form precipitation with and without dyes. Figure 15 illustrates that with increasing DTAB and SDS concentration, the T_K of DTAB-rich and SDS-rich was first increased rapidly and then drastically decreases. It is due to the electrostatic repulsion forms the local concentration of DTAB-rich and SDS-rich increase in the presence of SDS/DTAB in an aqueous medium. Therefore, DTAB-rich and SDS-rich mixed surfactants have no significant effect on the solubility of SDS and DTAB in liquid water at temperatures between 313.15 and 323.15 K, as shown in figure 15. Also, there is no remarkable rise in the solubility before temperature move towards the minimum temperature of the normal Krafft point 313.15 and 323.15 K. This also indicates that the Krafft point for DTAB-rich and SDS-rich mixed surfactants show different interaction activities, this condition does not shift to a temperature below 313.15 and 323.15 K.

4. Conclusion

The conductance and surface tension of SDS-rich and DTAB-rich mixtures in an aqueous medium at $T =$ 293.15, 298.15 and 303.15 K were used as a function of surfactant concentration. On increasing the concentration of surfactant and temperature, the conductance values are increased and CMC and α also increased. The CMC obtained by conductance and surface tension are close to each other. Also, ΔG_m^o and ΔH_m^o are found more negative with increment in temperature, while ΔS_m^o is found decreased with increase in temperature. The Krafft point is determined as the temperature where the solubility against temperature plot intersects with the specific conductance versus temperature graph. The surface tension is decreased at first with increment in the concentration of surfactant mixtures in water. DTAB-rich systems show the antagonistic interaction, whereas SDS-rich systems explore synergistic interaction. Hence the synergism in mixed micelle formation is present when mixed surfactants have a lower CMC than the individual surfactants. When the CMC is increased, then the value of Γ_{max} decreases and A_{min} followed the opposite trend. Similarly, when the CMC is increased, π_{cmc} increases while P and G_{ads}^o decreases. The ξ and PDI values are reflected in the dispersion and stability of the solution. An addition of dyes into SDS and DTAB-rich system increases the monodispersibility, which is confirmed by PDI measurement. The micellar size distribution of DTAB and SDS-rich surfactant analysed by DLS has confirmed their effective micellization for the stability of the solution with and without dyes. The binding and distribution constant of MO and MB between the aqueous phase and DTAB-rich micellar phase have been calculated efficiently.

References

1. Fan Y, Liu Y, Xi J, Guo R. 2011 Vesicle formation with amphiphilic chitosan derivatives and a conventional cationic surfactant in mixed systems. *J. Colloid Interface Sci.* **360**, 148–153. (doi:10.1016/j.jcis.2011.04.009)

2. Rub MA, Azum N, Asiri AM. 2017 Binary mixtures of sodium salt of ibuprofen and selected bile salts: interface, micellar, thermodynamic, and spectroscopic study. *J. Chem. Eng. Data* **62**, 3216–3228. (doi:10.1021/acs.jced.7b00298)

3. Cui Z-G, Canselier JP. 2001 Interfacial and aggregation properties of some anionic/cationic surfactant binary systems II. Mixed micelle formation and surface tension reduction effectiveness. *Colloid Polym. Sci.* **279**, 259–267. (doi:10.1007/s003960000420)

4. Kume G, Gallotti M, Nunes G. 2007 Review on anionic/cationic surfactant mixtures. *J. Surfactants Deterg.* **11**, 1–11. (doi:10.1007/s11743-007-1047-1)

5. Šegota S, Težak D. 2006 Spontaneous formation of vesicles. *Adv. Colloid Interface Sci.* **121**, 51–75. (doi:10.1016/j.cis.2006.01.002)

6. Rosen MJ, Kunjappu JT. 2012 *Surfactants and interfacial phenomenon*, 4th edn. New York NY: Wiley.

7. Sohrabi B, Gharibi H, Tajik B, Javadian S, Hashemianzadeh M. 2008 Molecular interactions of cationic and anionic surfactants in mixed monolayers and aggregates. *J. Phys. Chem. B* **112**, 14 869–14 876. (doi:10.1021/jp803105n)

8. Shiloach A, Blankschtein D. 1998 Predicting micellar solution properties of binary surfactant mixtures. *Langmuir* **14**, 1618–1636. (doi:10.1021/la971151r)

9. Tikariha D, Ghosh KK, Barbero N, Quagliotto P, Ghosh S. 2011 Micellization properties of mixed cationic gemini and cationic monomeric surfactants in aqueous-ethylene glycol mixture. *Colloids Surf. A* **381**, 61–69. (doi:10.1016/j.colsurfa.2011.03.027)

10. Javadian S, Gharibi H, Fallah HT. 2010 Adsorption and micellar properties of binary ionic/nonionic surfactant mixtures in ethylene glycol+water. *J. Chem. Eng. Data* **55**, 1122–1130. (doi:10.1021/je900564p.)

11. Caria A, Khan A. 1996 Phase behavior of catanionic surfactant mixtures:sodium bis(2-ethylhexyl)sulfosuccinate−didodecyldimethylammonium bromide−water system. *Langmuir* **12**, 6282–6290. (doi:10.1021/la960581z)

12. Silva BFB, Marques EF, Olsson U. 2011 Aqueous phase behavior of salt-free catanionic surfactants: the influence of solubility mismatch on spontaneous curvature and balance of forces. *Soft Matter* **7**, 225–236. (doi:10.1039/c0sm00477d)

13. Zana R, Lévy H, Danino D, Talmon Y, Kwetkat K. 1997 Mixed micellization of cetyltrimethylammonium bromide and an anionic dimeric (gemini) surfactant in aqueous solution. *Langmuir* **13**, 402–408. (doi:10.1021/la9606963)

14. Sohrabi B, Gharibi H, Javadian S, Hashemianzadeh M. 2007 A new model to study the phase transition from microstructures to nanostructures in ionic/ionic surfactants mixture. *J. Phys. Chem. B* **111**, 10 069–10 078. (doi:10.1021/jp073284j)

15. Yousefi A, Javadian S, Gharibi H, Kakemam J, Rashidi-Alavijeh M. 2011 Cosolvent effects on the spontaneous formation of nanorod vesicles in catanionic mixtures in the rich cationic region. *J. Phys. Chem. B* **115**, 8112–8121. (doi:10.1021/jp202199d)

16. Bhattarai A. 2015 Studies of the micellization of cationic–anionic surfactant systems in water and methanol–water mixed solvents. *J. Solution Chem.* **44**, 2090–2105. (doi:10.1007/s10953-015-0391-4)

17. Aslanzadeh S, Yousefi A. 2013 The effect of ethanol on nanostructures of mixed cationic and anionic surfactants. *J. Surfactants Deterg.* **17**, 709–716. (doi:10.1007/s11743-013-1548-z)

18. Sohrabi B, Eivazzadeh S, Sharifi A, Azadbakht R. 2015 Self-assembled catanionic surfactant mixtures in aqueous/ionic liquid systems. *J. Mol. Liq.* **211**, 754–760. (doi:10.1016/j.molliq.2015.07.025)

19. Xu W, Zhang Q, Wei H, Qin J, Yu L. 2015 Self-aggregation of catanionic surface active ionic liquids in aqueous solutions. *J. Surfactants Deterg.* **18**, 421–428. (doi:10.1007/s11743-014-1666-2)

20. Wang C, Cao XL, Guo L-L, Xu Z-C, Zhang L, Gong Q-T, Zhang L, Zhao L. 2016 Effect of molecular structure of catanionic surfactant mixtures on their interfacial properties. *Colloids Surf. A* **509**, 601–612. (doi:10.1016/j.colsurfa.2016.09.069)

21. Hao L-S, Deng Y-T, Zhou L-S, Ye H, Nan Y-Q, Hu P. 2012 Mixed micellization and the dissociated margules model for cationic/anionic surfactant systems. *J. Phys. Chem. B* **116**, 5213–5225. (doi:10.1021/jp300568k)

22. Bhattarai A, Pathak K, Dev B. 2017 Cationic and anionic surfactants interaction in water and methanol–water mixed solvent media. *J. Mol. Liq.* **229**, 153–160. (doi:10.1016/j.molliq.2016.12.021)

23. Sachin KM, Karpe S, Singh M, Bhattarai A. 2018 Physicochemical properties of dodecyltrimethylammonium bromide (DTAB) and sodiumdodecyl sulphate (SDS) rich surfactants in aqueous medium, at T = 293.15, 298.15, and 303.15 K. *Macromol. Symp.* **379**, 1700034. (doi:10.1002/masy.201700034)

24. Mehta SK, Chaudhary S, Bhasin KK. 2008 Self-assembly of cetylpyridinium chloride in water–DMF binary mixtures: a spectroscopic and physicochemical approach. *J. Colloid Interface Sci.* **321**, 426–433. (doi:10.1016/j.jcis.2008.02.043)

25. Ghosh S, Mondal S, Das S, Biswas R. 2012 Spectroscopic investigation of interaction between crystal violet and various surfactants (cationic, anionic, nonionic and gemini) in aqueous solution. *Fluid Phase Equilib.* **332**, 1–6. (doi:10.1016/j.fluid.2012.06.019)

26. Samiey B, Ashoori F. 2011 Kinetics of crystal violet fading in the presence of TX-100, DTAB and SDS. *Acta Chim. Slov.* **58**, 223–232.

27. Dey S, Mandal U, Mojumdar SS, Mandal AK, Bhattacharyya K. 2010 Diffusion of organic dyes in immobilized and free catanionic vesicles. *J. Phys. Chem. B* **114**, 15 506–15 511. (doi:10.1021/jp1068347)

28. Purkait M, DasGupta S, De S. 2004 Removal of dye from wastewater using micellar-enhanced ultrafiltration and recovery of surfactant. *Sep. Purif. Technol.* **37**, 81–92. (doi:10.1016/j.seppur.2003.08.005)

29. Ciocirlan O, Iulian O. 2008 Vapor pressure, density, viscosity and refractive index of dimethyl sulfoxide+1,4-dimethylbenzene system. *J. Serb. Chem. Soc.* **73**, 73–85. (doi:10.2298/jsc0801073c)

30. Kinart CM, Kinart WJ, Bald A. 1999 The measurements of the surface tension of mixtures of dimethyl sulfoxide with methyl, ethyl and propyl alcohols. *Phys. Chem. Liq.* **37**, 317–321. (doi:10.1080/00319109908031436)

31. Singh M. 2006 Survismeter — Type I and II for surface tension, viscosity measurements of liquids for academic, and research and development studies. *J. Biochem. Biophys. Methods* **67**, 151–161. (doi:10.1016/j.jbbm.2006.02.008)

32. Lind JE, Zwolenik JJ, Fuoss RM. 1959 Calibration of conductance cells at 25° with aqueous solutions of potassium chloride1. *J. Am. Chem. Soc.* **81**, 1557–1559. (doi:10.1021/ja01516a010)

33. Tsujii K. 1998 *Surface activity: principles, phenomena, and applications*. San Diego, CA: Academic Press.

34. Mukherjee I, Moulik SP, Rakshit AK. 2013 Tensiometric determination of Gibbs surface excess and micelle point: a critical revisit. *J. Colloid Interface Sci.* **394**, 329–336. (doi:10.1016/j.jcis.2012.12.004)

35. Niraula TP, Shah SK, Chatterjee SK, Bhattarai A. 2018 Effect of methanol on the surface tension and viscosity of sodiumdodecyl sulfate (SDS) in aqueous medium at 298.15–323.15 K. *Karbala Int. J. Mod. Sci.* **4**, 26–34. (doi:10.1016/j.kijoms.2017.10.004)

36. Shah SK, Chatterjee SK, Bhattarai A. 2015 The effect of methanol on the micellar properties of dodecyltrimethylammonium bromide (DTAB) in aqueous medium at different temperatures. *J. Surfactants Deterg.* **19**, 201–207. (doi:10.1007/s11743-015-1755-x)

37. Holland PM, Rubingh DN. 1992 Mixed surfactant systems. In *Mixed surfactant systems*, pp. 2–30. American Chemical Society.

38. Rosen MJ, Zhu BY. 1984 Synergism in binary mixtures of surfactants. *J. Colloid Interface Sci.* **99**, 427–434. (doi:10.1016/0021-9797(84)90123-2)

39. Chakraborty S, Chakraborty A, Saha SK. 2014 Tuning of physico-chemical characteristics of charged micelles by controlling head group interactions via hydrophobically and sterically

modified counter ions. *RSC Adv.* **4**, 32 579 – 32 587. (doi:10.1039/c4ra03937h)

40. Banipal TS, Sood AK. 2013 Mixed micellar and interfacial interactions of a triblock polymer (EO37PO56EO37) with a series of monomeric and dimeric surfactants. *J. Surfactants Deterg.* **16**, 881 – 891. (doi:10.1007/s11743-013-1516-7)

41. Sachin KM, Chandra A, Singh M. 2017 Nanodispersion of flavonoids in aqueous DMSO-BSA catalysed by cationic surfactants of variable alkyl chain at T= 298.15 to 308.15 K. *J. Mol. Liq.* **246**, 379 – 395. (doi:10.1016/j.molliq.2017.09.076)

42. Feky AAE *et al.* 2016 Use of biodegradation ratios in monitoring trend of biostimulated biodegradation in crude oil polluted soils. *Int. J. Sci. Technol. Res.* **5**, 179 – 184.

43. Li F, Rosen MJ, Sulthana SB. 2001 Surface properties of cationic gemini surfactants and their interaction with alkylglucoside or -maltoside surfactants. *Langmuir* **17**, 1037 – 1042. (doi:10.1021/la001162b)

44. Qin L, Wang X-H. 2017 Surface adsorption and thermodynamic properties of mixed system of ionic liquid surfactants with cetyltrimethyl ammonium bromide. *RSC Adv.* **7**, 51 426 – 51 435. (doi:10.1039/c7ra08915e)

45. Khan IA, Mohammad R, Alam MS. 2010 surface properties and mixed micellization of cationic gemini surfactants with ethyleneamines. *J. Chem. Eng. Data* **55**, 370 – 380. (doi:10.1021/je9003756)

46. Israelachvili JN, Mitchell DJ, Ninham BW. 1976 Theory of self-assembly of hydrocarbon amphiphiles into micelles and bilayers. *J. Chem. Soc. Faraday Trans.* **72**, 1525. (doi:10.1039/f29767201525)

47. Nagarajan R. 2002 Molecular packing parameter and surfactant self-assembly: the neglected role of the surfactant tail. *Langmuir* **18**, 31 – 38. (doi:10.1021/la010831y)

48. Sagisaka M, Saito T, Yoshizawa A, Rogers SE, Guittard F, Hill C, Blesic M. 2019 Water-in-CO₂ microemulsions stabilized by fluorinated cation-anion surfactant pairs. *Langmuir* **35**, 3445 – 3454. (doi:10.1021/acs.langmuir.8b03942)

49. Tanford C. 1980 *The hydrophobic effect: formation of micelles and biological membranes*. 2nd edn. New York, NY: Wiley.

50. Mukhim T, Ismail K. 2011 Aggregation, counter ion binding and adsorption behaviors of cetylpyridinium chloride in water/glycerol media at 25°C. *J. Surfactants Deterg.* **15**, 47 – 51. (doi:10.1007/s11743-011-1281-4)

51. Das D, Ismail K. 2008 Aggregation and adsorption properties of sodium dodecyl sulfate in water – acetamide mixtures. *J. Colloid Interface Sci.* **327**, 198 – 203. (doi:10.1016/j.jcis.2008.07.045)

52. Patel R, Khan AB, Dohare N, Ali MM, Rajor HK. 2015 Mixed micellization and interfacial properties of ionic liquid-type imidazolium gemini surfactant with amphiphilic drug amitriptyline hydrochloride and its thermodynamics. *J. Surfactants Deterg.* **18**, 719 – 728. (doi:10.1007/s11743-015-1709-3)

53. Basu RG, Chakraborty I, Ghosh S, Moulik SP. 2007 On mixed binary surfactant systems comprising MEGA 10 and alkyltrimethylammonium bromides: a detailed physicochemical study with a critical analysis. *J. Colloid Interface Sci.* **307**, 543 – 553. (doi:10.1016/j.jcis.2006.11.055)

54. Parekh P, Varade D, Parikh J, Bahadur P. 2011 Anionic – cationic mixed surfactant systems: micellar interaction of sodium dodecyl trioxyethylene sulfate with cationic gemini surfactants. *Colloids Surf. A* **385**, 111 – 120. (doi:10.1016/j.colsurfa.2011.05.057)

55. Nabi A, Tasneem S, Jesudason CG, Lee VS, Zain SBM. 2018 Study of interaction between cationic surfactant (CTAB) and paracetamol by electrical conductivity, tensiometric and spectroscopic methods. *J. Mol. Liq.* **256**, 100 – 107. (doi:10.1016/j.molliq.2018.01.185)

56. Sugihara G, Nagadome S, Oh S-W, Ko J-S. 2008 A review of recent studies on aqueous binary mixed surfactant systems. *J. Oleo. Sci.* **57**, 61 – 92. (doi:10.5650/jos.57.61)

57. Dan A, Ghosh S, Moulik SP. 2009 Physicochemistry of the interaction between inulin and alkyltrimethylammonium bromides in aqueous medium and the formed coacervates. *J. Phys. Chem. B* **113**, 8505 – 8513. (doi:10.1021/jp902641d)

58. Hao LS, Jia Y-F, Liu Q, Wang Y, Xu G-Y, Nan Y-Q. 2016 Influences of molecular structure of the cationic surfactant, additives and medium on the micellization of cationic/anionic surfactant mixed systems. *Colloids Surf. A* **511**, 91 – 104. (doi:10.1016/j.colsurfa.2016.09.054)

59. Varade D, Joshi T, Aswal VK, Goyal PS, Hassan PA, Bahadur P. 2005 Effect of salt on the micelles of cetyl pyridinium chloride. *Colloids Surf. A* **259**, 95 – 101. (doi:10.1016/j.colsurfa.2005.02.018)

60. Chatterjee A, Moulik SP, Sanyal SK, Mishra BK, Puri PM. 2001 Thermodynamics of micelle formation of ionic surfactants: a critical assessment for sodium dodecyl sulfate, cetyl pyridinium chloride and dioctyl sulfosuccinate (Na salt) by microcalorimetric, conductometric, and tensiometric measurements. *J. Phys. Chem. B* **105**, 12 823 – 12 831. (doi:10.1021/jp0123029)

61. Pan A, Naskar B, Prameela GKS, Phani Kumar BVN, Mandal AB, Bhattacharya SC, Moulik SP. 2012 Amphiphile behavior in mixed solvent media I: Self-aggregation and ion association of sodium dodecylsulfate in 1,4-dioxane – water and methanol – water media. *Langmuir* **28**, 13 830 – 13 843. (doi:10.1021/la303281d)

62. Herrington KL, Kaler EW, Miller DD, Zasadzinski JA, Chiruvolu S. 1993 Phase behavior of aqueous mixtures of dodecyltrimethylammonium bromide (DTAB) and sodium dodecyl sulfate (SDS). *J. Phys. Chem.* **97**, 13 792 – 13 802. (doi:10.1021/j100153a058)

63. Rub MA. 2019 Aggregation and interfacial phenomenon of amphiphilic drug under the influence of pharmaceutical excipients (green/biocompatible gemini surfactant). *PLoS ONE* **14**, e0211077. (doi:10.1371/journal.pone.0211077)

64. Mata J, Varade D, Bahadur P. 2005 Aggregation behavior of quaternary salt based cationic surfactants. *Thermochim. Acta* **428**, 147 – 155. (doi:10.1016/j.tca.2004.11.009)

65. Kamenka N, Chorro M, Talmon Y, Zana R. 1992 Study of mixed aggregates in aqueous solutions of sodium dodecyl sulfate and dodecyltrimethylammonium bromide. *Colloids Surf.* **67**, 213 – 222. (doi:10.1016/0166-6622(92)80300-Q)

66. Hao LS, Yang N, Xu G-Y, Jia Y-F, Liu Q, Nan Y-Q. 2016 Specific ion effects on the micellization of aqueous mixed cationic/anionic surfactant systems with various counterions. *Colloids Surf. A* **504**, 161 – 173. (doi:10.1016/j.colsurfa.2016.05.073)

67. Niraula TP, Chatterjee SK, Bhattarai A. 2018 Micellization of sodium dodecyl sulphate in presence and absence of alkali metal halides at different temperatures in water and methanol-water mixtures. *J. Mol. Liq.* **250**, 287 – 294. (doi:10.1016/j.molliq.2017.12.014)

68. del Rio JM, Prieto G, Sarmiento F, Mosquera V. 1995 Thermodynamics of micellization of N-octyltrimethylammonium bromide in different media. *Langmuir* **11**, 1511 – 1514. (doi:10.1021/la00005a018)

69. Chauhan S, Sharma K. 2014 Effect of temperature and additives on the critical micelle concentration and thermodynamics of micelle formation of sodium dodecyl benzene sulfonate and dodecyltrimethylammonium bromide in aqueous solution: a conductometric study. *J. Chem. Thermodyn.* **71**, 205 – 211. (doi:10.1016/j.jct.2013.12.019)

70. Ghosh DKK, Quagliotto P. 2009 Micellization behavior of [C-16-4-C-16], 2Br(-) gemini surfactant in binary aqueous-solvent mixtures. *Indian J. Chem.* **48A**, 1522 – 1526.

71. Norvaišas P, Petrauskas V, Matulis D. 2012 Thermodynamics of cationic and anionic surfactant interaction. *J. Phys. Chem. B* **116**, 2138 – 2144. (doi:10.1021/jp2095888)

72. Rub MA, Asiri AM, Naqvi AZ, Rahman MM, Khan SB, Din K. 2013 Mixed micellization between amphiphilic drug promethazine hydrochloride and cationic surfactant (conventional as well as gemini). *J. Mol. Liq.* **177**, 19 – 25. (doi:10.1016/j.molliq.2012.10.003)

73. Talhout R, Engberts JBFN. 1997 Self-assembly in mixtures of sodium alkyl sulfates and alkyltrimethylammonium bromides: aggregation behavior and catalytic properties. *Langmuir* **13**, 5001 – 5006. (doi:10.1021/la970388k)

74. Mitra D, Chakraborty I, Bhattacharya SC, Moulik SP. 2007 Interfacial and solution properties of tetraalkylammonium bromides and their sodium dodecyl sulfate interacted products: a detailed physicochemical study. *Langmuir* **23**, 3049 – 3061. (doi:10.1021/la062830h)

75. Sohrabi B, Poorgholami-Bejarpasi N, Nayeri N. 2014 Dispersion of carbon nanotubes using mixed surfactants: experimental and molecular dynamics simulation studies. *J. Phys. Chem. B* **118**, 3094 – 3103. (doi:10.1021/jp407532j)

76. Liu R, Yoshida H, Narisawa S, Fujita S, Arai M. 2012 The dispersion of TiO₂ modified by the accumulation of CO₂ molecules in water: an effective medium for photocatalytic H₂

77. Zaghbani N, Dhahbi M, Hafiane A. 2011 Spectral study of Eriochrome Blue Black R in different cationic surfactant solutions. *Spectrochim. Acta A* **79**, 1528–1531. (doi:10.1016/j.saa.2011.05.011)

78. Tunç S, Duman O, Kancı B. 2012 Spectrophotometric investigation of the interactions between cationic dye (C.I. Basic Yellow 2) and anionic surfactant (sodium dioctylsulfosuccinate) in the premicellar and micellar region. *Dyes Pigm.* **94**, 233–238. (doi:10.1016/j.dyepig.2012.01.016)

79. Kansal S, Singh M, Sud D. 2007 Studies on photodegradation of two commercial dyes in aqueous phase using different photocatalysts. *J. Hazard. Mater.* **141**, 581–590. (doi:10.1016/j.jhazmat.2006.07.035)

80. Wang YH, Liu XQ, Meng GY. 2008 Preparation and properties of supported 100% titania ceramic membranes. *Mater. Res. Bull.* **43**, 1480–1491. (doi:10.1016/j.materresbull.2007.06.041)

81. Magid LJ, Konno K, Martin CA. 1981 Binding of phenols to inverted micelles and microemulsion aggregates. *J. Phys. Chem.* **85**, 1434–1439. (doi:10.1021/j150610a031)

82. Hunter RJ. 1981 *Zeta potential in colloid science*. London, UK: Academic Press. See https://www. elsevier.com/books/zeta-potential-in-colloid-science/hunter/978-0-12-361961-7.

83. Dobrowolska ME, Koper GJM. 2014 Optimal ionic strength for nonionically initiated polymerization. *Soft Matter* **10**, 1151. (doi:10.1039/c3sm51998h)

84. Savvin SB, Chernova RK, Shtykov SN. 1991 *Poverkhnostno-aktivnye veshchestva(surfactants)*. Moscow, Russia: Nauka.

85. Stepanov BI. 1977 *Vvedenie v khimiyu i tekhnologiyu organicheskikh krasitelei (Introduction to chemistry and technology of organic dyes)*. Moscow, Russia: Khimiya.

86. Naeem K, Shah SS, Shah SWH, Laghari GM. 2000 Solubilization of cationic hemicyanine dyesin anionic surfactant micelles: a partitioning study. *Monatshefte Fuer Chemie/Chem. Mon.* **131**, 761. (doi:10.1007/s007060050023)

87. Karukstis KK, Litz JP, Garber MB, Angell LM, Korir GK. 2010 A spectral approach to determine location and orientation of azo dyes within surfactant aggregates. *Spectrochim. Acta A* **75**, 1354–1361. (doi:10.1016/j.saa.2009.12.087)

88. Bales BL, Benrraou M, Zana R. 2002 Krafft temperature and micelle ionization of aqueous solutions of cesium dodecyl sulfate. *J. Phys. Chem. B* **106**, 9033–9035. (doi:10.1021/jp021297l)

89. King WE. 1979 *Principles of solution and solubility, Kozo Shinoda* (translated in collaboration with Paul Becher). New York, NY: Marcel Dekker.

90. Oakes J, Gratton P. 2003 Solubilisation of dyes by surfactant micelles. Part 2: molecular interactions of azo dyes with cationic and zwitterionic surfactants. *Coloration Technol.* **119**, 100–107. (doi:10.1111/j.1478-4408.2003.tb00157.x)

91. Zhang JS, Lee S, Lee JW. 2007 Does SDS micellize under methane hydrate-forming conditions below the normal Krafft point? *J. Colloid Interface Sci.* **315**, 313–318. (doi:10.1016/j.jcis.2007.06.049)

92. Gayet P, Dicharry C, Marion G, Graciaa A, Lachaise J, Nesterov A. 2005 Experimental determination of methane hydrate dissociation curve up to 55 MPa by using a small amount of surfactant as hydrate promoter. *Chem. Eng. Sci.* **60**, 5751–5758. (doi:10.1016/j.ces.2005.04.069)

93. Khan F, Rub MA, Azum N, Asiri AM. 2018 Mixtures of antidepressant amphiphilic drug imipramine hydrochloride and anionic surfactant: micellar and thermodynamic investigation. *J. Phys. Org. Chem.* **31**, e3812. (doi:10.1002/poc.3812)